Stereoselective Coupling of Prochiral Radicals with a Chiral C_2-Symmetric Nitroxide

Rebecca Braslau,*,† Neeta Naik,† and Hendrik Zipse‡

Contribution from the Department of Chemistry and Biochemistry, University of California, Santa Cruz, California 95064, and the Department of Chemistry, Ludwig-Maximilians-Universität, 81377 München, Germany

Received February 11, 2000

Abstract: The coupling reaction between a chiral C_2-symmetric nitroxide, *trans*-2,5-dimethyl-2,5-diphenylpyrrolidin-1-oxyl (DPPO; **1)**, and a series of stabilized secondary prochiral radicals was studied to determine the factors that affect stereoselectivity. Both steric and electronic perturbations on the selectivity by the substituents of the prochiral radical were observed. The effects of temperature, solvent polarity, and solvent viscosity were examined. High selectivity for reactions carried out in solvents of low viscosity provides evidence for the formation of an encounter complex on the reaction path. Ab initio calculations on simplified model systems predict the C−O−N angle of attack to be greater than 110° at a carbon−oxygen bond-forming distance of approximately 2.2 Å, although no transition state was found.

Introduction

Free radicals are highly reactive species which can be used to effect organic transformations under mild conditions. Advantages of radical over ionic reactions include chemoselectivity in the tolerance of a wide range of functionalities without the need for protecting groups, the general absence of solvent effects, and the predictive power afforded by numerous measured rate constants for radical reactions. Over the past two decades, extensive use has been made of radical intermediates in connective transformations to assemble target skeletons.[1] More recently, advances in the control of stereochemistry in radical reactions have been demonstrated.[2,3] Not surprisingly, radical intermediates are subject to the same types of conformational analysis and predictive transition states as their ionic counterparts. We have been engaged in a research program to study the ability of nonbonded, noncoordinated chiral reagents to discriminate between the two faces of a prochiral carbon radical. Only a few stereochemical studies of intermolecular reactions involving prochiral radicals have been reported, which include hydrogen abstraction reactions from optically active reagents[4] and the addition of prochiral radicals to optically active unsaturated substrates[5] (or to activated alkenes coordinated to optically active Lewis acids[6]). The third intermolecular reaction possibility, coupling reactions between prochiral radicals and chiral radical partners, has not been addressed.[7] Nitroxides are persistent species[8] and are highly effective traps for carbon radicals,[9] with coupling rate constants on the order of 10^7 to 10^9 M^{-1} s^{-1} at room temperature.[10] We have previously published stereochemical studies on the coupling of chiral, optically active steroid or terpene-derived nitroxides with prochiral carbon radicals.[11,12] Although moderate to good stereoselectivity was observed, in the best cases, analysis of the products was challenging due to dynamic behavior in the NMR spectra of the *N*-alkoxyamine products. Herein we describe stereoselectivity studies in the reaction of a chiral C_2-symmetric nitroxide with a variety of prochiral carbon radicals. The ratios of the product *N*-alkoxyamines were readily determined by integration of the proton NMR spectra. This made possible a series of experiments to probe the stereoselectivity in terms of both steric and electronic effects by varying substituents on the prochiral radical and examining the temperature and solvent effects. As these reactions probe the stereoselectivity of two radicals approaching each other without

† Department of Chemistry and Biochemistry, University of California, Santa Cruz.

‡ Department of Chemistry, Ludwig-Maximilians-Universität.

(1) (a) Curran, D. P. *Synthesis* **1988**, 417−439. (b) Curran, D. P. *Synthesis* **1988**, 489−513. (c) Curran, D. P. *Chem. Rev.* **1991**, *91*, 1237−1286.

(2) Curran, D. P.; Porter, N. A.; Giese, B. *Stereochemistry of Radical Reactions*; VCH: New York, 1996.

(3) Sibi, M. P.; Porter, N. A. *Acc. Chem. Res.* **1999**, *32*, 163−171.

(4) (a) Nanni, D.; Curran, D. P. *Tetrahedron: Asymmetry* **1996**, *7*, 2417−2422. (b) Blumenstein, M.; Schwarzkopf, K.; Metzger, J. O. *Angew. Chem., Int. Ed. Engl.* **1997**, *36*, 235−236. (c) Schwarzkopf, K.; Blumenstein, M.; Hayen, A.; Metzger, J. O. *Eur. J. Org. Chem.* **1998**, *177*, 7−181. (d) Haque, M. B.; Roberts, B. P. *Tetrahedron Lett.* **1996**, *37*, 9123−9126. (e) Haque, M. B.; Roberts, B. P.; Tocher, D. A. *J. Chem. Soc., Perkin Trans. 1* **1998**, 2881−2889. (f) Dakternieks, D.; Dunn, K.; Perchyonok, V. T.; Schiesser, C. H. *J. Chem. Soc., Chem. Commun.* **1999**, 1665−1666. (g) A tin hydride bearing (L)-borneol prepared in situ: Schumann, H.; Pachaly, B.; Schuetze, B. C. *J. Organomet. Chem.* **1984**, *265*, 145−152.

(5) (a) Fukuzawa, S.; Seki, K.; Tatsuzawa, M.; Mutoh, K. *J. Am. Chem. Soc.* **1997**, *119*, 1482−1483. (b) Sibi, M. Personal communication.

(6) Mikami, K.; Yamaoka, M. *Tetrahedron Lett.* **1998**, *39*, 4501−4504.

(7) (a) For a discussion of diastereoselective radical−radical self-dimerizations and stereoselectivity in geminate radical pair recombinations, see: ref 2, pp 242−250. (b) Enantiomeric recoginition in radical recombination has been studied in the context of the 1,2-Wittig rearrangement: Tomooka, K.; Igarashi, T.; Nakai, T. *Tetrahedron Lett.* **1993**, *34*, 8139−8142.

(8) For a discussion of persistent radicals reacting with transient radicals, see: Fischer, H. *J. Am. Chem. Soc.* **1986**, *108*, 3925−3927.

(9) Griller, D.; Ingold, K. U. *Acc. Chem. Res.* **1976**, *8*, 13−19.

(10) (a) Bowry, V. W.; Ingold, K. U. *J. Am. Chem. Soc.* **1992**, *114*, 4992−4996. (b) Chateauneuf, J.; Lusztyk, J.; Ingold, K. U. *J. Org. Chem.* **1988**, *53*, 1629−1632. (c) Arends, I. W. C. E.; Mulder, P.; Clark, K. B.; Wayner, D. D. M. *J. Phys. Chem.* **1995**, *99*, 8182−8189.

(11) (a) Braslau, R.; Burrill, L. C.; Mahal, L. K.; Wedeking, T. *Ang. Chem., Int. Ed. Eng.* **1997**, *36*, 237−238. (b) Braslau, R.; Burrill, L. C.; Chaplinski, V.; Howden, R.; Papa, P. W. *Tetrahedron: Asymmetry* **1997**, *8*, 3209−3212.

(12) Stereoselective coupling of acyclic chiral nitroxides with prochiral radicals will be reported separately. Braslau, R.; Chaplinski, V. Manuscript in preparation.

10.1021/ja000520u CCC: $19.00
Published on Web 08/12/2000

Scheme 1

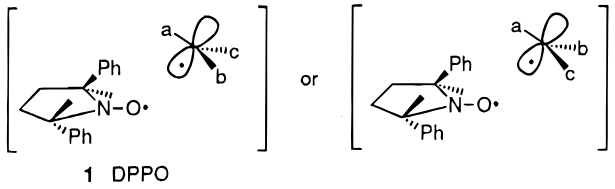

1 DPPO

the presence of chelating agents, such as metals or Lewis acids, these studies provide an opportunity to study the fundamental behavior of free radical reactivity in solution.

Results and Discussion

Choice of Chiral Nitroxide. The nitroxide *trans*-2,5-dimethyl-2,5-diphenyl- pyrrolidin-1-oxyl (DPPO;[13] **1**) was chosen for this study. It was prepared and used in racemic form following a slight modification of the synthetic scheme developed by Puts and Sogah[13a,14] (see Scheme 18 in the Supporting Information).

The C_2-symmetry of the nitroxide ensures that the N−O π bond has enantiotopic faces, thus simplifying the number of stereochemical approaches in the key coupling reaction. Since both faces of the N−O π bond are the same, there are only two possibilities: reaction of the nitroxide from one or the other enantiotopic face of the prochiral carbon radical (Scheme 1). In reactions of a non-C_2-symmetric chiral nitroxide, the nitroxide three electron N−O π bond has two diastereotopic faces, each of which will have different reactivity to the prochiral radical. Because of the cyclic structure of DPPO, the nitroxide is conformationally restrained and cannot exist as a collection of rotamer populations. This simplifies the reaction pathway to only two possible trajectories.

Generation of Prochiral Radicals. Prochiral radicals were generated using stoichiometric methods under oxidizing conditions which were compatible with the nitroxide functionality. Three different methods were utilized: the oxidation of stabilized carbanions with $CuCl_2$,[15] the Mn(salen) method developed by Hawker,[16] and the oxidation of benzyl hydrazines with lead oxide.[15]

Metal-mediated oxidation of carbanions to radicals using copper salts[17] has been used synthetically, such as in the oxidative coupling of enolate anions. Iron salts[18] have been used as well; for example, Jahn has utilized ferrocenium hexafluorophosphonate as a mild single-electron oxidant to form carbon radicals.[19] In the case of the copper-mediated oxidative coupling of two enolates, mechanistic studies by Porter[20] indicate that radical addition to a metal enolate is probably more realistic than true radical−radical coupling. In previous studies from our labs, 2,2,6,6-tetramethylpiperidinyloxy (TEMPO) has been coupled with carbon radicals generated from lithium ester enolates.[15] Generation of prochiral radical **2** from ester or nitrile substrates followed by coupling with DPPO gave the expected *N*-alkoxyamine products (Scheme 2). In all experiments, the chiral nitroxide was the limiting reagent. The lithium anions were generated at −78 °C, using LDA in THF, and added by cannula to a solution of DPPO and anhydrous $CuCl_2$. In the first experiment, using *tert*-butyl propionate, quenching of the reaction mixture at −78 °C gave the same results as allowing the reaction mixture to warm to room temperature overnight. All subsequent reactions were allowed to warm overnight as the standard protocol.

The selectivities observed in this series of coupling reactions were modest; however, the diastereoselectivity ratios (dr) were reproducible. In comparing the first two entries of Table 1, the bulky *tert*-butyl ester substituted prochiral radical was much more selective than the carbomethoxy analogue: dr = 1.9:1 compared to 1.1:1. Comparing entries 2 and 3, substitution of the methyl group by the larger cyclohexyl group again gave increased selectivity: dr = 2.0:1 (cyclohexyl) as compared to

Scheme 2

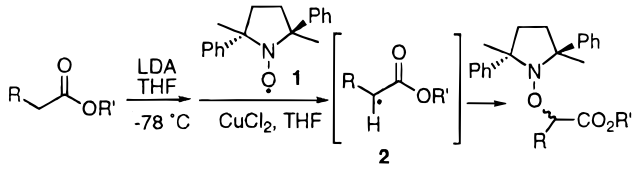

Table 1. Stereochemical Results from Coupling of Prochiral Radicals Generated by $CuCl_2$ Oxidation of Stabilized Carbanions with the Nitroxide DPPO

	Me	*c*-C_6H_{11}	Ph	CO_2Me	CN
A Values	1.7	2.2	3.0	1.2 -1.3	0.2

Entry			Yield	Selectivity (dr)
1	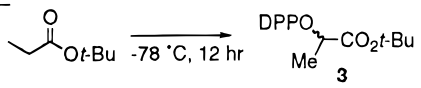	**3**	80%	1.9:1
2	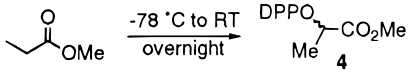	**4**	55%	1.1:1
3	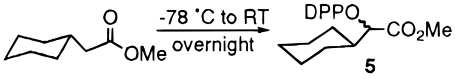	**5**	76%	2.0:1
4	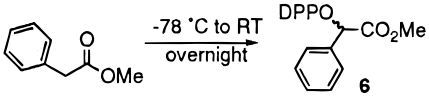	**6**	72%	1.4:1
5	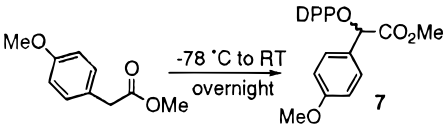	**7**	72%	1.6:1
6	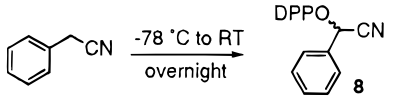	**8**	50%	1.3:1
7	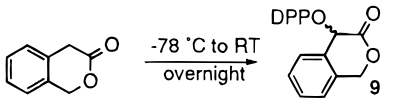	**9**	45%	1.3:1

(13) (a) Puts, R. S.; Sogah D. Y. *Macromolecules* **1996**, *29*, 3323−3325. (b) Benfaremo, N.; Steenbock, M.; Klapper, M.; Müllen, K.; Enkelmann, V.; Cabrera, K. *Liebigs Ann. Chem.* **1996**, 1413−1415. (c) Einhorn, J.; Einhorn, C.; Ratajczak, F.; Gautier-Luneau, I.; Pierre, J.-L. *J. Org. Chem.* **1997**, *62*, 9385−9388.

(14) Kornblum, N.; Wade, P. A. *J. Org. Chem.* **1973**, *38*, 1418−1420.

(15) Braslau, R.; Burrill, L. C.; Siano, M.; Naik, N.; Howden, R. K.; Mahal, L. K. *Macromolecules* **1997**, *30*, 6445−6450.

(16) Dao, J.; Benoit, D.; Hawker, C. J. *J. Polym. Sci., Part A: Polym. Chem.* **1998**, *36*, 2161−2167.

(17) (a) Falck, J. R.; Mekonnen, B.; Yu, J. R.; Lai, J. Y. *J. Am. Chem. Soc.* **1996**, *118*, 6096−6097. (b) You, S.; Neuenschwander, M. *Chimia* **1992**, *46*, 377−380.

(18) (a) Poupart, M.-A.; Lassalle, G.; Paquette, L. A. *Org. Synth.* **1990**, *69*, 173−179. (b) Ramig, K.; Kuzemko, M. A.; McNamara, K.; Cohen, T. *J. Org. Chem.* **1992**, *57*, 1968−1969. (c) Schwartz, E. B.; Knobler, C. B.; Cram, D. J. *J. Am. Chem. Soc.* **1992**, *114*, 10775−10784.

(19) Jahn, U. *J. Org. Chem.* **1998**, *63*, 7130−7131.

(20) (a) Porter, N. A.; Rosenstein, I. J. *Tetrahedron Lett.* **1993**, *34*, 7865−7868. (b) Porter, N. A.; Su, Q.; Harp, J. J.; Rosenstein, I. J.; McPhail, A. T. *Tetrahedron Lett.* **1993**, *34*, 4457−4460.

Scheme 3

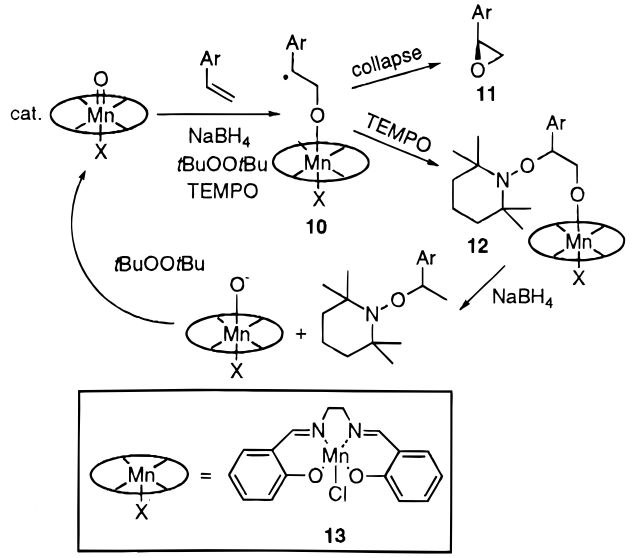

1.1:1 (methyl). Although the phenyl group has a larger "*A* value"[21] than the cyclohexyl group, it is flat: in the prochiral radical, the π electrons will be coplanar with the SOMO in order to delocalize the unpaired electron density. Thus, the effective size of the phenyl substituent is less than the standard "*A* value" for phenyl, which assumes a freely rotating aromatic ring. Comparison of entries 4 and 5 examines the perturbation by introducing an electron-donating substituent on the aromatic ring. Substitution in the para position was chosen to minimize steric effects upon introduction of a methoxy group. A small increase of dr = 1.6:1as compared to dr = 1.4:1 was seen upon introduction of this electron-donating group. In another example, the very small nitrile group was used in place of an ester substituent. Comparing entries 4 and 6 shows that the selectivity decreases slightly in going from carbomethoxy, "*A* value" of 1.2, to the much smaller nitrile, "*A* value" of 0.2: dr = 1.4:1 as compared to dr = 1.3:1. The data from Table 1 imply that increasing the steric bulk[22] of one of the substituents on the prochiral radical tends to lead to higher diastereoselectivity.

To probe the electronic contribution to the stereoselectivity, prochiral radicals bearing para-substituted aromatic rings were examined using the Mn(salen) method developed by Hawker to prepare *N*-alkoxyamines as initiators for nitroxide mediated "living" free radical polymerization.[16] This method utilizes the catalyst systems developed by Jacobsen and Katsuki for asymmetric epoxidations.[23] In the Hawker protocol, a manganese oxo species reacts with styrene to generate a carbon radical **10**, which is trapped by a nitroxide before collapse to epoxide **11** can take place (Scheme 3). Sodium borohydride reduces the coupled product **12** in situ to give the phenethyl *N*-alkoxyamine and to free the manganese complex to return to the catalytic cycle. In Hawker's work, the commercially available optically active Jacobsen manganese salen complex has been used. However, in this study, the use of a chiral manganese complex would make the two faces of the carbon radical **10** diastereotopic rather than enantiotopic and could bias the stereoselectivity as

Scheme 4

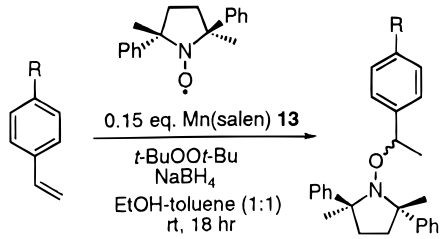

cmpd	R	Yield	dr	σ_ρ value
14	H	56%	3.4:1	0.00
15	NO_2	75%	2.4:1	-0.57
16	NH_2	39%	2.9:1	+0.81

Scheme 5

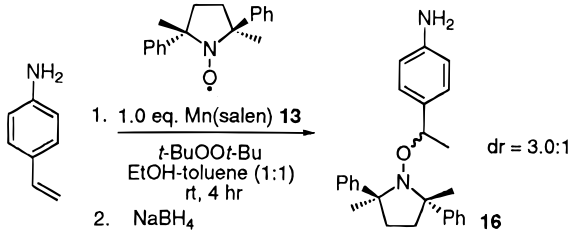

well as lead to kinetic resolution of the racemic DPPO. To make the prochiral radical **10** stereochemically neutral, an achiral Mn(salen) catalyst **13** was prepared in one step[24] from manganese diacetate tetrahydrate and *N*,*N*′-bis(salicylidiene)ethylenediamine (see Scheme 19 in the Supporting Information). With this achiral catalyst in hand, DPPO was coupled to an electron-poor styrene, an electron-rich styrene, and the parent unsubstituted styrene (Scheme 4). These reactions were carried out at room temperature.

As can be seen from the results, both the electron-withdrawing nitro group (σ_ρ value = −0.57)[25] and the electron-donating amine group (σ_ρ value = +0.81) lead to a diminution of the selectivity compared to that of the unsubstituted styrene (R═H, σ_ρ value = 0). To rule out the possibility that the aniline nitrogen was coordinated to a boron species derived from the sodium borohydride, the reaction was repeated with a stoichiometric amount of the Mn(salen) reagent, followed by a subsequent reduction step with sodium borohydride (Scheme 5). The stereoselectivity was not significantly changed (dr = 3.0:1 as compared to dr = 2.9:1).

Recent calculations by Svensson et al.[26] on the Mn(salen) epoxidation pathway indicate that reaction between the manganese oxo species and alkene begins on the triplet surface, followed by spin change to the quintet surface, which then leads to the quintet epoxide complexed manganese product without a barrier. This implies that intermediate **10** is not a typical benzyl radical but rather has a significantly different reactivity profile. Since no epoxide product was found in the presence of DPPO, we assume that the nitroxide intercepts the triplet species before spin-state crossing can occur. They also found that alkene substituents influence the timing of the spin-crossing, with electron-withdrawing substituents causing spin-crossing to occur later in the reaction path. In epoxidation reactions, this allows more carbon−carbon bond rotation to occur in intermediate **10**,

(21) Eliel, E. L.; Wilen, S. H.; Mander, L. N. *Stereochemistry of Organic Compounds*; Wiley: New York, 1994; p 695.

(22) For a study on the effect of steric bulk on the *rate* of nitroxides coupling with carbon radicals, see: Iwao, K.; Sakakibara, K.; Hirota, M. *J. Comput. Chem.* **1998**, *19*, 215−221.

(23) (a) Finney, N. S.; Pospisil, P. J.; Chang, S.; Palucki, M.; Konsler, R. G.; Hansen, K. B.; Jacobsen, E. N. *Angew. Chem., Int. Ed. Engl.* **1997**, *36*, 1720−1723 and references therein. (b) Katsuki, T. *Coord. Chem. Rev.* **1995**, *140*, 189−214.

(24) Palucki, M.; Finney, N. S.; Pospisil, P. J.; Guler, M. L.; Ishida, T.; Jacobsen, E. N. *J. Am. Chem. Soc.* **1998**, *120*, 948−954.

(25) March, J. *Advanced Organic Chemistry: Reactions, Mechanisms, and Structure*; Wiley: New York, 1992; p 280.

(26) Linde, C.; Åermark, B.; Norrby, P.-O.; Svensson, M. *J. Am. Chem. Soc.* **1999**, *121*, 5083−5084.

Scheme 6

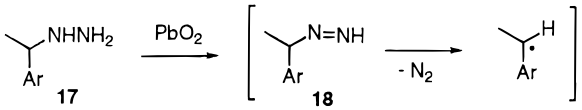

Scheme 7

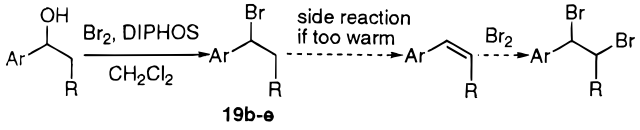

leading to a mixture of *cis* and *trans* epoxides from a *cis* olefin substrate. In our reactions, both electron-donating and electron-withdrawing substituents on the aromatic ring are expected to help stabilize a benzylic radical intermediate and will lower the rotational barrier. Thus, the lower selectivities for the two substituted styrene substrates may derive from nitroxide trapping a less favorable mixture of rotational conformers compared to the unsubstituted styrene substrate.

The third method used to generate stoichiometric radicals under mild conditions is the lead dioxide oxidation of alkyl hydrazines **17**, utilized by Corey to add carbon radicals to nitroso compounds.[27] A diazene intermediate **18** forms, which decomposes to the carbon radical with the extrusion of dinitrogen (Scheme 6). This is consistent with the work of Meyers, in which a diazene formed by an alternate route, anionic desilylation, decomposes to a free radical which has been trapped by TEMPO.[28]

We have demonstrated that benzyl hydrazines are easily formed from benzyl bromides by S_N2 displacement using sonication to facilitate mixing of the two reactants.[15] Benzyl bromides **19b**−**e**, other than commercially available phenethyl bromide **19a**, were prepared via bromination of the corresponding benzyl alcohols using the bromine 1,2-bis(diphenylphosphino)ethane (DIPHOS) procedure developed by Schmidt and Brooks.[29] Use of DIPHOS is advantageous over the more commonly used triphenylphosphine, as the phosphine oxide byproduct is easily removed by a simple precipitation−filtration procedure, employing the prescribed solvent mixture. Thus, the sensitive benzyl bromides can be obtained cleanly in high yield without resorting to silica gel chromatography. However, in two cases, the standard procedure gave 1,2-dibromides as the major products. These presumably form by elimination of HBr from the desired benzyl bromide followed by addition of bromine to the styrene intermediate (Scheme 7). This undesired dibromination could be avoided by carrying out the reaction between −15 and 15 °C instead of allowing the reactions to warm to room temperature (see Table 4 in the Supporting Information).

The resulting benzyl bromides were then reacted with hydrazine, followed by treatment with lead dioxide in the presence of DPPO at −78 °C, and allowed to warm to room temperature to give the *N*-alkoxyamine products (Scheme 8, Table 2). The selectivities observed in the hydrazine/lead dioxide method were much better than those observed with the LDA/$CuCl_2$ method, presumably due to the slower coupling rate of benzyl versus α-ester-substituted radicals with nitroxides.[30] The

Scheme 8

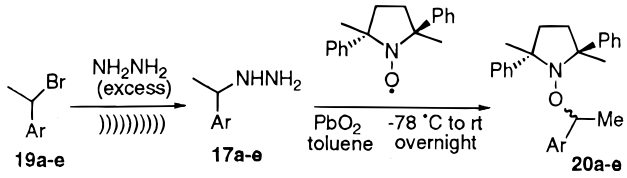

Table 2. Stereochemical Results from Coupling of Prochiral Radicals Generated by Oxidation of Benzyl Hydrazines Derived from Benzyl Bromides with the Nitroxide DPPO

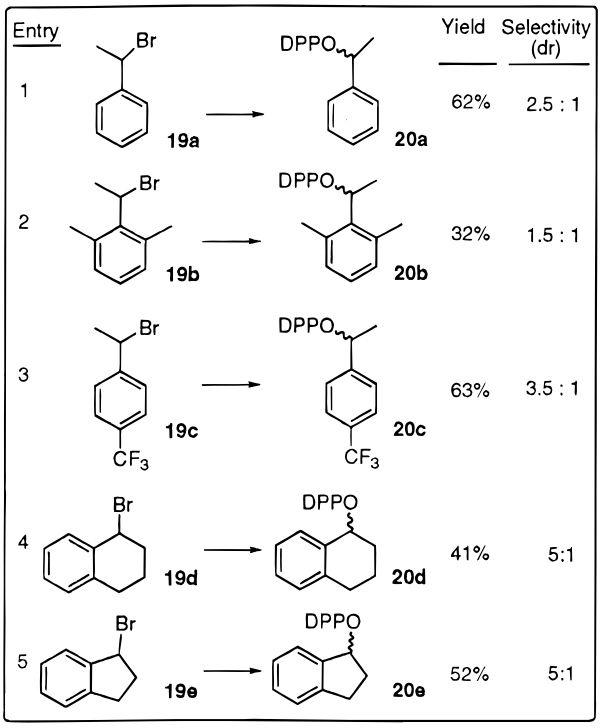

parent 1-phenethyl radical gave a dr of 2.5:1. In entry 2, the sterically very hindered di-*ortho*-methyl-substituted radical gave a dr of only 1.5:1. This decrease in selectivity is a reflection of slight pyramidalization due to severe steric interactions between the two *ortho*-methyl substituents on the benzene ring with the methyl and hydrogen at the prochiral radical center. The pyramidalization causes the substituents on the prochiral radical to be pointed away from the incoming nitroxide, in contrast to the planar orientation of substituents on the 1-phenethyl radical. The electron-poor *p*-trifluoromethyl-substituted benzyl radical in entry 3 gave a slightly improved diastereoselectivity of 3.5:1. The 1-tetralinyl and 1-indanyl radicals gave the best diastereoselectivity of the series: dr = 5:1. Structurally, the 1-tetralinyl radical is very similar to the 1-phenethyl radical; the only difference is that the "methyl group" is tied back into a rigid ring. This enhanced selectivity of a cyclic radical is very similar to that observed by Guindon in diastereoselective hydrogen transfer reactions.[31] He reported a significant increase in diastereoselectivity when an acyclic radical was transformed into an endocyclic radical intermediate by chelation with a Lewis acid. Similarly, in this work, the endocyclic tetralinyl and indanyl radicals were more selective than the acyclic 1-phenethyl radical. As these cyclic radicals gave good diastereoselectivity, the 1-tetralinyl case was chosen for further studies.

We have recently prepared another interesting C_2-symmetric chiral nitroxide in our laboratory, *trans*-1,3-dimethyl-1,3-

(27) (a) Corey, E. J.; Gross, A. W. *Tetrahedron Lett.* **1984**, *25*, 491−494. (b) Corey, E. J.; Gross, A. W. *J. Org. Chem.* **1985**, *50*, 5391−5393.

(28) Myers, A. G.; Movassaghi, M. *J. Am. Chem. Soc.* **1998**, *120*, 8891−8892.

(29) Schmidt, S. P.; Brooks, D. W. *Tetrahedron Lett.* **1987**, *28*, 767−768.

(30) Keoshkerian, B.; Georges, M.; Quinlan, M.; Veregin, R.; Goodbrand, B. *Macromolecules* **1998**, *31*, 7559−7561.

(31) Guindon, Y.; Liu, Z. P.; Jung, G. *J. Am. Chem. Soc.* **1997**, *119*, 9289−9290.

Scheme 9

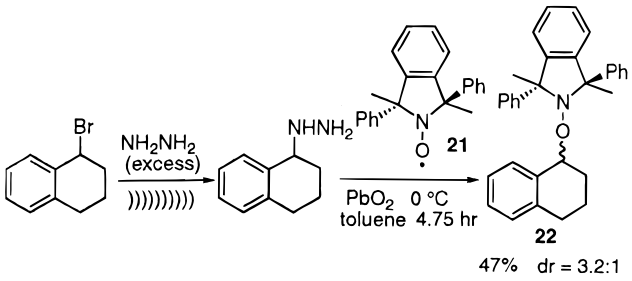

Scheme 10

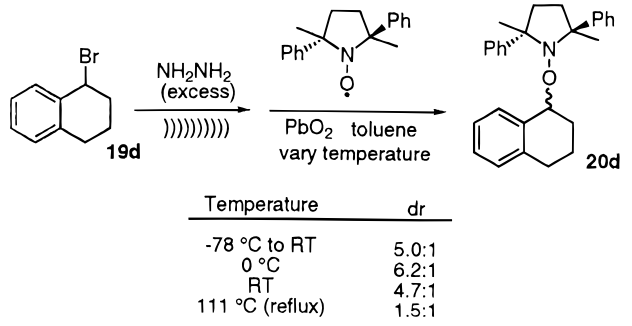

Temperature	dr
-78 °C to RT	5.0:1
0 °C	6.2:1
RT	4.7:1
111 °C (reflux)	1.5:1

Scheme 11

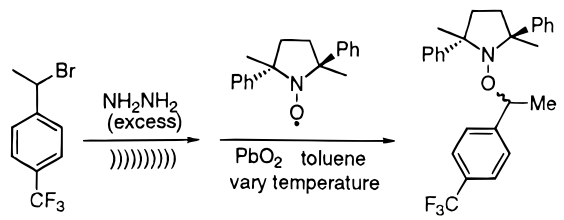

Temperature	dr
-78 °C to rt, overnight	3.5:1
0 °C, 4 hr	4.1:1

diphenylisoindoline-1-oxyl (**21**), and showed that it reacted with 1-phenethyl radical at 0 °C to give 81% of the *N*-alkoxyamine product with a dr = 2.2:1.[32] When it was coupled with 1-tetralinyl radical at 0 °C, the *N*-alkoxyamine product **22** was obtained in a 3.2:1 diastereomeric ratio (Scheme 9).

Temperature Effects. The coupling of the 1-tetralinyl radical with DPPO was studied to determine the effect of temperature on the stereoselectivity. The reaction was carried out at four different temperatures: −78 °C to room temperature, 0 °C, room temperature, and at reflux in toluene. The results obtained are shown in Scheme 10. The reaction run at a constant 0 °C was more selective than the reaction started at −78 °C and allowed to warm to room temperature. This same phenomenon was observed in using the 1-(4-trifluoromethylphenyl)ethyl radical (Scheme 11). This led us to question at what temperature carbon radicals are formed under our reaction conditions. Thus, ESR experiments were undertaken to monitor the disappearance of the nitroxide signal.

ESR Studies with TEMPO. As a model reaction, 1-phenethyl radical was generated from the corresponding benzyl hydrazine in the presence of TEMPO at low temperature in an NMR tube and monitored by ESR[33] (Scheme 12). The temperature was raised in increments: the disappearance of the nitroxide signal is indicative of carbon radical formation.

Scheme 12

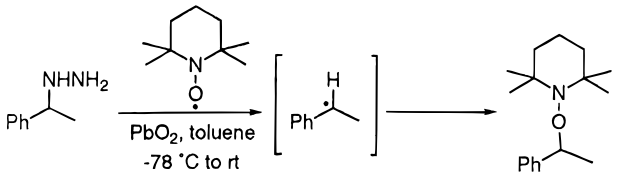

Scheme 13

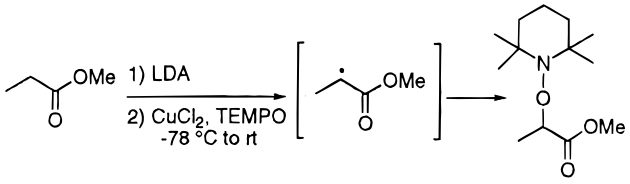

The reaction was started at −78 °C; ESR spectra were acquired every 30 min. After 2 h, no significant change in the TEMPO signal had been detected. The temperature was raised to −38 °C and the TEMPO signal monitored every 15 min for 2.5 h. Again, no change was detected in the nitroxide ESR signal. The temperature was then raised to 2 °C, and the TEMPO signal monitored every 10 min. At this temperature, the ESR indicated an ∼50% decrease in nitroxide concentration every 30 min period. The temperature was then raised to 22 °C, and ESR spectra were measured at 5 min intervals, revealing an even more rapid decrease in the nitroxide signal. Thus, the benzyl hydrazine reacts to generate benzyl radical at a temperature somewhere between −38 and 2 °C. This result explains the poorer diastereoselectivities observed for experiments started at −78 °C and warmed to room temperature compared to experiments held at 0 °C. In the −78 °C to room-temperature experiments, the reaction does not proceed at temperatures much lower than 0 °C; however, when the prochiral radical is finally generated, the reaction vessel does not linger at 0 °C but quickly approaches room temperature.

A similar ESR study was carried out for radicals generated by the Cu(II) oxidation of stabilized lithium anions. In this case, the coupling of the lithium enolate of methyl propionate with TEMPO was examined (Scheme 13). This reaction was carried out in a 0.2 mm o.d. ESR tube. At −78 °C, no change in the nitroxide signal[34] was observed after 2 h. At −38 °C, the TEMPO signal was no longer a clean triplet but had broadened out, possibly because of interaction with copper ion. Integration of the nitroxide signal showed a 60% decrease, indicating that the radical formed in the range between −78 and −38 °C.

Solvent Effects. Kinetic studies by Beckwith, Bowry, and Ingold[35] using both laser flash photolysis and the radical "clock" method have shown that solvent polarity affects the rate of the coupling reaction between nitroxides and carbon radicals. The rates were found to be strongly correlated with nitroxide solvation, as determined by the solvent's effect on the nitrogen hyperfine splitting in the ESR. Nitroxides have a significant dipole moment, resulting from a contribution from the dipolar canonical resonance structure which localizes the unpaired electron on the nitrogen (Scheme 14). Polar solvents will stabilize the dipolar form, enhancing the distribution of unpaired spin on nitrogen. In order for coupling of a nitroxide with a

(32) Braslau, R.; Chaplinski, V.; Goodson, P. *J. Org. Chem.* **1998**, *63*, 9857−9864.

(33) The variable temperature ESR spectra can be obtained from the Supporting Information.

(34) The ESR spectra at −78 °C and −38 °C can be obtained from the Supporting Information.

(35) Beckwith, A. L. J.; Bowry, V. W.; Ingold, K. U. *J. Am. Chem. Soc.* **1992**, *114*, 4983−4992.

Scheme 14

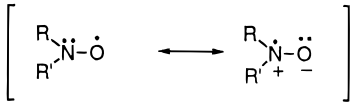

Scheme 15

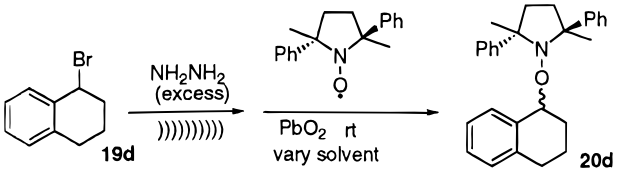

Effect of Solvent Polarity on the Stereoselectivity

Solvent	Dielectric constant	dr
toluene	2.4	4.7:1
THF	7.4	4.9:1
EtOH	24.3	5.1:1
MeOH	32.6	4.6:1

carbon radical to occur, polar solvent molecules must be displaced, leading to slower rate constants in comparison to reaction in a nonpolar solvent. In addition to polar solvent effects, coupling reactions were found to be unexpectedly fast in hydroxylic solvents.[36] This was termed the "anomalous" nitroxide radical trapping effect. It is postulated that a directional hydrogen bond between the nitroxide and the solvent is responsible for this rate enhancement, as stabilization of the dipolar canonical resonance structure by hydroxylic solvents can occur with an orientation that does not impede the carbon radical coupling. Solvent polarity also has an influence on the bond dissociation enthalpies of *N*-alkoxyamines, as determined by photoaccoustic calorimetry.[37] This is again due to the difference in solvation between the *N*-alkoxyamine and the nitroxide in polar solvents. Since both the rate of *N*-alkoxyamine formation and N−O bond strength are affected by solvent polarity, we examined the diastereoselectivity of the coupling reaction in both hydroxylic and nonhydroxylic solvents of varying polarity.

The 1-tetralinyl radical displayed good selectivity in coupling with DPPO; thus, it was utilized for probing the effects of solvent polarity (Scheme 15). Four solvents with similar viscosity but increasing polarity[38] were examined: toluene, tetrahydrofuran, ethanol, and methanol. Surprisingly, no significant trend was observed in the diastereoselectivity: the average dr for all four solvents is 4.8:1, which is not far from the value of the least polar of the group, toluene, or the most polar of the group, methanol.

Solvent viscosity is also known to influence the rate of nitroxide coupling with carbon radicals, although this effect is generally smaller than the influence of solvent polarity.[33] We examined the diastereoselectivity in a series of solvents of increasing viscosity[39] (Scheme 16). Here the results were dramatic. In the least viscous solvent, diethyl ether, the selectivity at room temperature was the best of the series: dr = 5.2:1. At

Scheme 16

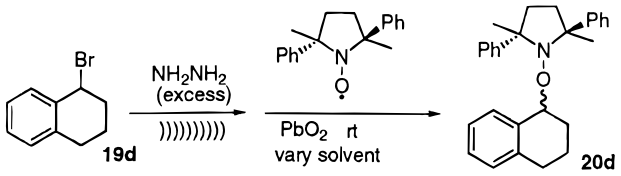

Effect of Solvent Viscosity on the Stereoselectivity

Solvent	Viscosity(cp)	dr
Et_2O	0.233	5.2:1
toluene	0.590	4.7:1
t-BuOH	3.897	3.9:1
ethylene glycol	19.9	2.1:1

the other extreme, the very viscous ethylene glycol solvent resulted in a far less selective reaction: dr = 2.1:1.

To understand these findings, insight into the details of the carbon radical−nitroxide coupling process is necessary. It is well-known that the rates of stabilized carbon radical coupling reactions with nitroxides are significantly slower than radical−radical self-recombination processes, which are generally considered close to diffusion controlled. Even the rates of radical−radical self-reactions are affected by solvent viscosity. Typically, reaction rates decrease with more viscous solvents, providing evidence for rate determination by formation of diffusive encounter pairs.[40] Fischer has probed radical−radical self-reactions by studying the product distribution between dimerization and disproportionation as a function of solvent viscosity. The ratio between dimers and products of disproportionation is controlled by the ability of the radical pairs to reorient themselves between repeated collisions. For example, with *tert*-butyl radicals, the geometry required for dimerization, coincidence of the principal axis in a parallel orientation, is much more restrictive than that required for disproportionation. As solvent viscosity increases, reorientational motions are inhibited. Thus, the ratio of disproportionation is much higher in viscous solvents compared to dimerization.

In carbon radical coupling reactions with nitroxides, slower than diffusion controlled reactions have been attributed to an entropic barrier lying between the caged singlet radical pair and the *N*-alkoxyamine product.[35] Beckwith, Bowry, and Ingold speculated that this entropic barrier arises from the need to localize the unpaired electron on the nitroxide oxygen before coupling can occur. With delocalized benzyl radicals, a component of the barrier is also due to the need to localize spin at the benzylic carbon before coupling can proceed. Earlier work along these same lines using laser flash photolysis[41] compared nitroxide trapping of carbon radicals with similar steric demands but differing resonance stabilization. They found that more stabilized radicals react significantly more slowly. For example, the rate of TEMPO trapping at 20 °C by benzyl radical was 4.9×10^8 M^{-1} s^{-1} and the rate by 1-naphthylmethyl radical was 8.2×10^7 M^{-1} s^{-1}. In this case, the steric demands of the two radicals are approximately the same, whereas the 1-naphthylmethyl radical has approximately 4.5 kcal/mol greater resonance

(36) Valgimigli, L.; Banks, J. T.; Ingold, K. U.; Lusztyk, J. *J. Am. Chem. Soc.* **1995**, *117*, 9966−9971.

(37) Ciriano, M. V.; Korth, H.-G.; van Scheppingen, W. B.; Mulder, P. *J. Am. Chem. Soc.* **1999**, *121*, 6375−6381.

(38) All values were obtained from the *Handbook of Chemistry and Physics*, 56th ed.; CRC Press: Boca Raton, FL, 1975; pp E-56−E-57, except for THF: Carvajal, C.; Tolle, K. J.; Smid, J.; Szwarc, M. *J. Am. Chem. Soc.* **1965**, *87*, 5548−5553.

(39) Viscosity values for (a) Et_2O and toluene: *Handbook of Chemistry and Physics*, 56th ed.; CRC Press: Boca Raton, FL, 1975; pp F-52−F-55. (b) *t*-BuOH: Viswanth, D. S.; Natarajan, G. *Data Book on the Viscosity of Liquids*; Hemisphere Pub. Corp.: New York, 1989. (c) THF: Carvajal, C.; Tolle, K. J.; Smid, J.; Szwarc, M. *J. Am. Chem. Soc.* **1965**, *87*, 5548−5553.

(40) Fischer, H.; Paul, H. *Acc. Chem. Res.* **1987**, *20*, 200−206.

(41) Chateauneuf, J.; Lusztyk, J.; Ingold, K. U. *J. Org. Chem.* **1988**, *53*, 1629−1632.

stabilization. Even the least stabilized carbon radicals (primary alkyl and cyclopropyl) react about 10 times slower than diffusion-controlled reactions. By studying the temperature dependence of these reactions, it was concluded that this is due to an unfavorable entropy of activation. Mulder and Wayner[10c] have also studied the rate constants for benzylic radicals coupling with TEMPO. They too postulate the formation of a loose-encounter complex followed by a solvent-dependent rearrangement to form the *N*-alkoxyamine product. They noted that the rate constants decrease as the N−O bond in the coupled product becomes weaker, and concluded that both steric factors and thermodynamic considerations influence the dynamics in this complex recombination system. In recent work from the Mulder labs investigating the thermal stability of *N*-alkoxyamines,[37] the coupling reaction of benzyl radical with TEMPO is again described as occurring through a reversible encounter of the two radical species to from a short-lived intermediate. Subsequent rearrangement through an activated process gives the *N*-alkoxyamine. Fischer[42] has recently studied the rate constants of cumyl radical coupling with TEMPO under conditions of kinetic isolation and determined an $E_a = 0.9$ kcal/mol with a reaction entropy of $\Delta S = 38$ kcal mol^{-1} K^{-1}. Similarly, Scaiano[43] has determined an $E_a = 2.3$ kcal/mol for 1-phenethyl radical coupling with TEMPO using Ingold's kinetic data.[10a]

With this model of an intermediary encounter complex along the pathway to the formation of the *N*-alkoxyamine, the higher diastereoselectivity observed in the less viscous solvents for our coupling reactions of the chiral DPPO nitroxide can be understood. With less viscous solvents, the prochiral radical has more opportunity to reorient itself in a looser-encounter complex to achieve a more favorable coupling product, as compared to that in a more viscous, tighter-encounter complex. Clearly the rate of the coupling, which is influenced by solvent polarity, is less important in the diastereoselectivity than the looseness or tightness of the solvent cage around the encounter complex.

Dynamic NMR of *N*-Alkoxyamine Products. Dynamic NMR characteristics were observed in the room temperature ^{1}H and ^{13}C spectra of all *N*-alkoxyamines derived from DPPO. The signals for the methyl and phenyl groups on the pyrrolidine ring and the methylene of the pyrrolidine ring were shorter and broader than normal signals and were seen as nonequivalent pairs of peaks.[44] This type of dynamic NMR behavior has been previously reported for a number of *N*-alkoxyamines, based on the piperidine[45] and isoindoline[46] ring systems. The temperature dependence of these NMR spectra is attributed to a conformational process involving ring inversion, nitrogen inversion, and rotation about the nitrogen−oxygen bond. The five-membered rings of the isoindoline and the pyrrolidine-based *N*-alkoxyamines have a less pronounced conformational preference compared to that of the six-membered piperidine rings. Thus,

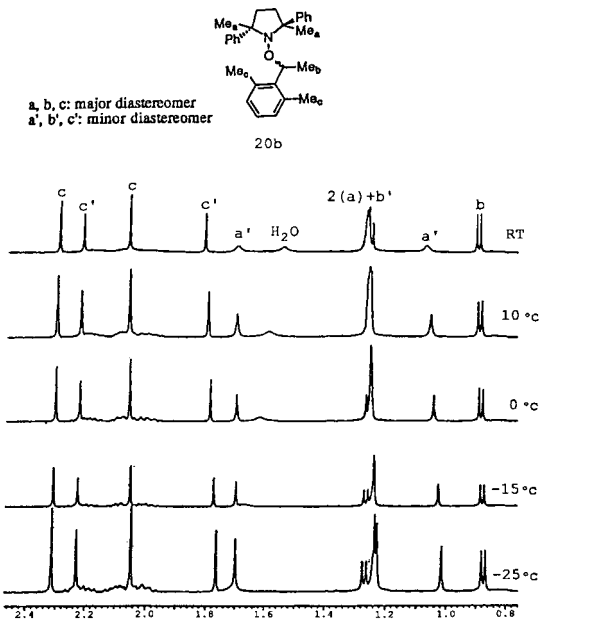

Figure 1. Variable temperature ^{1}H NMR spectra of the *N*-alkoxyamine **20b** in $CDCl_3$ showing sharpening of signals of the pyrrolidine ring methyl groups at lower temperature.

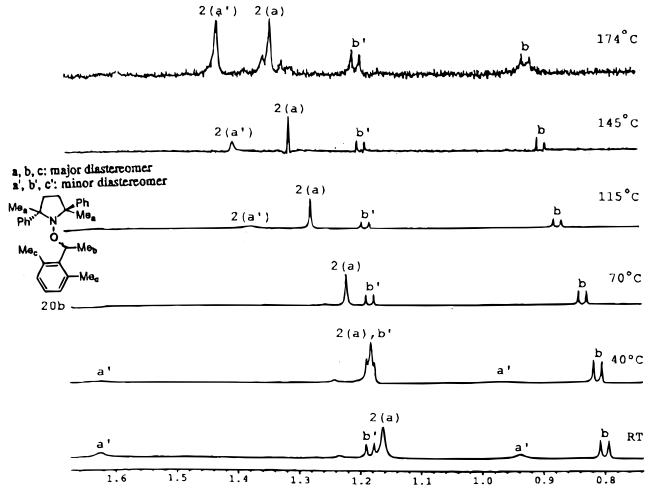

Figure 2. Variable temperature ^{1}H NMR spectra of the *N*-alkoxyamine **20b** in DMSO-d_6 showing coalescence of the pyrrolidine ring methyl groups at high temperature.

the dynamic behavior is attributed to hindered nitrogen inversion and nitrogen−oxygen bond rotation in the pyrrolidinine systems.

Multitemperature ^{1}H NMR studies were carried out on one of the DPPO diastereomeric coupling products, *N*-alkoxyamine **20b**. The methyl groups on the pyrrolidine ring should be homotopic because of the C_2-symmetry and, thus, would be expected to show only one signal for each diastereomer. However, due to hindered nitrogen inversion and hindered rotation around the nitrogen−oxygen bond, four methyl signals were seen for the mixture of two diastereomers. At room temperature in $CDCl_3$, the methyl groups of the minor diastereomer are seen as a set of short, broad signals separated by 0.7 ppm, whereas the methyl groups of the major diastereomer are seen together as a larger, broad peak (Figure 1). When cooled to −25 °C, all of the methyl signals sharpen, and the two peaks from the major diastereomer can be discerned. In a separate series of experiments in DMSO-d_6, the temperature was raised over a series of steps (Figure 2). At 115 °C, the methyl signals corresponding to the minor

(42) (a) Kothe, T.; Marque, S.; Martschke, R.; Popov, M.; Fischer, H. *J. Chem. Soc., Perkin Trans. 2* **1998**, 1553−1559. (b) Fischer, H. *J. Polym. Sci., Part A: Polym. Chem.* **1999**, *37*, 1885−1901.

(43) Skene, W. G.; Belt, S. T.; Connolly, J. J.; Hahn, P.; Scaiano, J. C. *Macromolecules* **1998**, *31*, 9103−9105.

(44) For a typical example of ^{1}H and ^{13}C NMR spectra illustrating this dynamic behavior, see the Supporting Information.

(45) (a) Anderson, J. E.; Corrie, J. E. T. *J. Chem. Soc., Perkin Trans. 2* **1992**, 1027−1031. (b) Anderson, J. E.; Casarini, D.; Corrie, J. E. T.; Lunazzi, L. *J. Chem. Soc., Perkin Trans. 2* **1993**, 1299−1304. (c) Brown, T. M.; Cooksey, C. J.; Crich, D.; Dronsfield, A. T.; Ellis, R. *J. Chem. Soc., Perkin Trans. 1* **1993**, 2131−2136.

(46) (a) Busfield, W. K.; Jenkins, I. A.; Thang, S. H.; Moad, G.; Rizzardo, E.; Solomon, D. H. *J. Chem. Soc., Chem. Commun.* **1985**, 1249−1250. (b) Beckwith, A. L. J.; Bowry, V. W.; Moad, G. *J. Org. Chem.* **1988**, *53*, 1632−1641.

Scheme 17

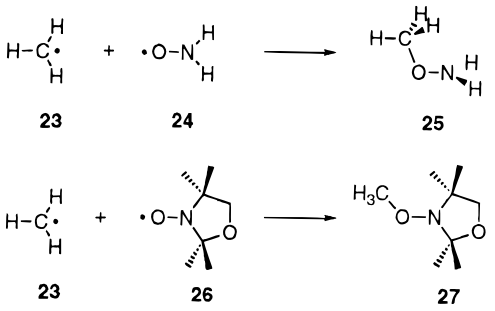

diastereomer coalesced. At 174 °C, each diastereomer displays a single, sharp methyl signal.

It is noteworthy that the two diastereomers are expected to interconvert at temperatures in the 85−100 °C range, by way of bond homolysis,[47] to form nitroxide and secondary benzyl radical, followed by recombination. This is the underlying basis for nitroxide-mediated "living" free radical polymerization, which has been studied by Puts and Sogah[13a] using the nitroxide DPPO. In their work, polymerization of styrene with DPPO was investigated both experimentally and by semiempirical PM3 calculations on the coupling reaction with 1-phenethyl radical. Experimentally, they found that polymerization proceeded (albeit slowly) at 90 °C but was completely suppressed at 75 °C. Their calculations gave a rough estimate of $\Delta(\Delta H^{\ddagger}) = 1.08$ kcal/mol for the difference in enthalpies between the formation of the (*R*,*R*)−*S* and (*R*,*R*)−*R* diastereomers of **20a**, with the later being favored. Making a crude assumption that $\Delta(\Delta S^{\ddagger}) = 0$ for the formation of the two diastereomers, this value predicts the formation of diastereomers in a 7.4:1 ratio at 0 °C, a 6.2:1 ratio at room temperature, and a 4.1:1 ratio in refluxing toluene. Our results gave a ratio of 2.5:1 for the reaction started at −78 °C and allowed to warm to room temperature, in which the coupling probably occurred over an actual range of 0 °C to room temperature. The results of 1-tetralinyl radical coupling with DPPO in reactions held at constant temperatures (a 6.2:1 ratio at 0 °C, a 4.7:1 ratio at room temperature, and a 1.5:1 ratio in refluxing toluene) indicate that the value derived by Puts and Sogah is not unreasonable.

Theoretical Studies on the Geometry of Approach. As a carbon radical and a nitroxide come together to form an *N*-alkoxyamine, the carbon radical approaches the three-electron π-bond of the nitroxide in a pathway reminiscent of the Bürgi−Dunitz trajectory for nucleophilic addition to a carbonyl π-bond.[48] To probe the energetics and geometry of approach of carbon radicals reacting with nitroxides, a series of calculations were carried out.

To evaluate which theoretical methods give a reliable description of the recombination reaction between nitroxides and carbon-centered radicals, we first took a detailed look at a small model system. Thus, the recombination of methyl radical **23** and nitroxide radical **24** to give methoxy amine **25** was examined (Scheme 17).

Of particular interest were those methods that not only yielded reliable reaction energetics but also allowed for geometry optimization of larger model systems. A first test of the performance of various methods was the correct prediction of the reaction energy for the recombination of **23** and **24**. As no experimental value is currently available for this system, all reactants were optimized using the hybrid density functional Becke3LYP[49] in combination with the polarized VDZ basis set by Ahlrichs et al.[50,51] In keeping with the terminology used in Gaussian 98, this level of theory will be termed "B3LYP/SVP". A similar level of theory has recently been used by Tordo et al.[52] in studies of the $H_2NO^{\bullet}$ + $^{\bullet}H$ recombination reaction. The reaction energies of **23** coupling with **24** calculated at this level of theory are −49.3 and −56.9 kcal/mol with and without accounting for differences in zero-point vibrational energy (Table 3). Using these geometries, a more reliable estimate of the reaction energy was obtained by single-point calculations at the UCCSD(T) level of theory in combination with various correlation consistent basis sets by Dunning et al.[53] Quite surprisingly, the results obtained at the coupled cluster level are quite similar to those obtained with B3LYP/SVP. Moreover, the CCSD(T) results appear to depend only marginally on the choice of the basis set. The best estimate of the reaction energy at 0 K is obtained at the UCCSD(T)/aug-cc-pVTZ//B3LYP/SVP level of theory in combination with the unscaled B3LYP/SVP zero-point vibrational energy and amounts to $\Delta E_{rxn}(0\ K) = -54.3$ kcal/mol.

Table 3. Reaction Energy for the Recombination of Methyl Radical **23** with Nitroxide Radical **24** To Give Methoxyamine **25**[a]

level of theory	ΔE_{rxn}
UB3LYP/SVP	−56.9
UB3LYP/SVP + ΔZPE	−49.3
UCCSD(T)/cc-pVDZ//B3LYP/SVP	−60.0
UCCSD(T)/aug-cc-pVDZ//B3LYP/SVP	−59.4
UCCSD(T)/cc-pVTZ//B3LYP/SVP	−61.9
UCCSD(T)/aug-cc-pVTZ//B3LYP/SVP	−61.9
UB3LYP/6-31G(d)	−58.6
UB3LYP/6-31G(d) + ΔZPE	−51.2
UB3LYP/DZVP	−56.7
UB3LYP/DZVP + ΔZPE	−48.2
UBLYP/DZVP	−55.4
UBLYP/DZVP + ΔZPE	−48.2

[a] All energies are in kcal/mol.

The basis set dependence of the B3LYP result was also tested by choosing two smaller basis sets: the economical 6-31G(d) basis set, as well as the even smaller DZVP basis set specifically optimized for density functional methods by Godbout et al.[54] The reaction energies calculated with these smaller basis sets are still very close to the B3LYP/SVP result; thus, we conclude that, at least the reaction energies can be calculated with good accuracy with even a medium-sized basis set. An even more

(47) Moad, G.; Rizzardo, E. *Macromolecules* **1995**, *28*, 8722−8728.
(48) Eliel, E. L.; Wilen S. H.; Mander, L. N. *Stereochemistry of Organic Compounds*; Wiley−Interscience: New York, 1994; p 877.
(49) (a) Becke, A. D. *J. Chem. Phys.* **1993**, *98*, 5648−5652. (b) Lee, C.; Yang, W.; Parr, R. G. *Phys. Rev. B* **1988**, *37*, 785−789. (c) Hertwig, R. H.; Koch, W. *J. Comput. Chem.* **1995**, *16*, 576−585.
(50) Schaefer, A.; Horn, H.; Ahlrichs, R. *J. Chem. Phys.* **1992**, *97*, 2571−2577.
(51) All calculations have been performed with Gaussian 98, Revision A.7, Frisch, M. J.; Trucks, G. W.; Schlegel, H. B.; Scuseria, G. E.; Robb, M. A.; Cheeseman, J. R.; Zakrzewski, V. G.; Montgomery, J. A., Jr.; Stratmann, R. E.; Burant, J. C.; Dapprich, S.; Millam, J. M.; Daniels, A. D.; Kudin, K. N.; Strain, M. C.; Farkas, O.; Tomasi, J.; Barone, V.; Cossi, M.; Cammi, R.; Mennucci, B.; Pomelli, C.; Adamo, C.; Clifford, S.; Ochterski, J.; Petersson, G. A.; Ayala, P. Y.; Cui, Q.; Morokuma, K.; Malick, D. K.; Rabuck, A. D.; Raghavachari, K.; Foresman, J. B.; Cioslowski, J.; Ortiz, J. V.; Baboul, A. G.; Stefanov, B. B.; Liu, G.; Liashenko, A.; Piskorz, P.; Komaromi, I.; Gomperts, R.; Martin, R. L.; Fox, D. J.; Keith, T.; Al-Laham, M. A.; Peng, C. Y.; Nanayakkara, A.; Gonzalez, C.; Challacombe, M.; Gill, P. M. W.; Johnson, B.; Chen, W.; Wong, M. W.; Andres, J. L.; Gonzalez, C.; Head-Gordon, M.; Replogle, E. S.; Pople, J. A. Gaussian, Inc.: Pittsburgh, PA, 1998.
(52) Marsal, P.; Roche, M.; Tordo, P.; de Sainte Claire, P. D. *J. Phys. Chem. A* **1999**, *103*, 2899−2905.
(53) (a) Dunning, T. H. Jr. *J. Chem. Phys.* **1989**, *90*, 1007−1023. (b) Kendall, R. A.; Dunning, T. H. Jr.; Harrison, R. J. *J. Chem. Phys.* **1992**, *96*, 6769−6806. (c) Davidson, E. R. *Chem. Phys. Lett.* **1996**, *220*, 514−518.
(54) Godbout, N.; Salahub, D. R.; Andzelm, J.; Wimmer, E. *Can. J. Chem.* **1992**, *70*, 560−571.

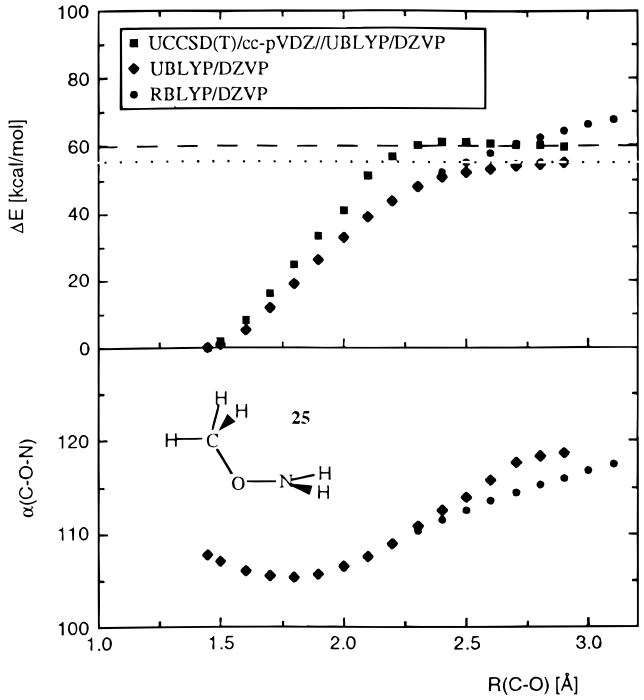

Figure 3. Relative energies as well as C−O−N angle deformation along the pathway for dissociation of **25** into methyl radical **23** and nitroxide radical **24**.

economical procedure involves the combination of a gradient-corrected pure density functional without admixture of Hartree−Fock exchange, such as the BLYP functional with the DZVP basis set. The reaction energy calculated at this level of theory is only slightly smaller than with the B3LYP functional, and we have therefore decided to perform all calculations for the larger systems at this level of theory.

The next important consideration concerns the recombination process. It is widely known that a correct description of the recombination process requires a multiconfigurational treatment. However, such an approach is not feasible for geometry optimizations of even moderately large systems. We have therefore used the same density functional methods employed before to follow the reaction pathway for recombination of **23** and **24**.

Because we did not expect to find a transition state for the recombination process, we started the investigation of the potential energy surface by incrementally stretching the C−O bond in product **25** (0.1 Å per step) while all other structural parameters were allowed to vary. The relaxed potential energy scan obtained in this way at the BLYP/DZVP level of theory is shown in Figure 3. Using restricted Kohn−Sham orbitals as in RBLYP, the energy of the system increases steadily, surpassing the energy of the separate reactants **23** and **24** (shown as a dotted line in Figure 1) beyond a C−O distance of approximately 2.5 Å. It is in this region that the use of unrestricted Kohn−Sham orbitals starts to lead to an energetically more favorable solution. Moreover, with increasing C−O bond distance, the UBLYP curve smoothly approaches the energy of the separate reactants (shown as a dotted line in Figure 3). On the downside, the UBLYP solution ceases to describe a singlet state beyond 3.0 Å, as the $<S^2>$ expectation values are larger than 1.0 at these distances. A very similar picture emerges upon using the hybrid B3LYP functional (not shown), and it therefore appears that the use of a hybrid density functional does not yield a decisive advantage in this case. To obtain more reliable reference values, a series of UCCSD(T)/cc-pVDZ single-point calculations were performed using the UBLYP geometries. The UCCSD(T) level of theory has performed exceedingly well in earlier studies of bond dissociation processes, even in combination with medium-sized basis sets.[55] The UCCSD(T) dissociation curve is slightly steeper as compared to that of the UBLYP level of theory, but also flattens out after reaching the energy of the separate products (shown as a dashed line in Figure 3). The energy of the system at 2.4 Å exceeds that of the separate reactants by 1.1 kcal/mol and, thus, indicates a slight recombination barrier. However, the accuracy of the UCCSD(T) level of theory is of similar magnitude to this 1.1 kcal/mol barrier. Thus, we conclude that all theoretical methods examined in this study indicate that recombination of radicals **23** and **24** proceeds with a negligible enthalpic barrier. One of the important structural characteristics of the C−O bond formation process concerns the angle of attack (lower part of Figure 3). Both the RBLYP and the UBLYP methods agree, in that the C−O−N angle is larger than 105° throughout the addition process. The angle of attack varies around 117° at large C−O distances, and the two methods only differ in how quickly this initial value approaches smaller values upon shortening the C−O bond.

How relevant are these findings for recombination reactions involving sterically demanding chiral nitroxides? To answer this question, to at least some extent, we have also studied the reaction between methyl radical **23** and nitroxide **26** (Scheme 17). Nitroxide **26** was chosen as a simple model for the chiral steroidal doxyl nitroxide used in our earlier experiments.[11a] These radicals recombine to give product **27**. The main difference between this and the first reaction is the enhanced steric bulk present by virtue of the four methyl substituents in **26**. As a consequence of these steric effects, the reaction exothermicity is reduced to −42.4 kcal/mol at the BLYP/DZVP level of theory. Accounting for differences in zero-point vibrational energy, this value is reduced to −36.3 kcal/mol. Using the latter value, this represents a reduction of around 12 kcal/mol as compared to the recombination reaction involving nitroxide **24**.

To determine whether the steric effects would be sufficiently large to cause formation of an enthalpic barrier along the recombination pathway, the recombination of **23** and **26** was followed from a C−O distance of 3.0 Å, using the same theoretical approach as before (Figure 4). The RBLYP/UBLYP instability occurs at the same C−O distance as seen in the previous case. In this instance we did not follow the RBLYP curve beyond 2.5 Å, but instead concentrated on the UBLYP results. For C−O distances larger than 2.5 Å, the UBLYP energies are almost identical to the sum of the energies of the two reactants (shown as a dotted line in Figure 4). Even with the enhanced steric bulk present in **26**, no transition state could be found for the recombination process on the potential energy surface. Variations in the C−O−N angle along the recombination pathway appear to be similar to that seen with **24** (Figure 3) and **26** (Figure 4). It is only at the longer C−O bond distances around 3.0 Å that the angle of attack is somewhat larger for **26**, with values around 130°. If one assumes that an enthalpic barrier, if it exists, would be located at C−O distances around 2.2 Å,[56] it is safe to conclude that the angle of attack would be larger than 110°. A three-dimensional representation of **27** at this bond distance is shown in Figure 5. The C−O−N bond

(55) Chen, W.; Schlegel, H. B. *J. Chem. Phys.* **1994**, *101*, 5957−5968.

(56) This choice is motivated by the CCSD(T) results which indicate that the onset of C−O bond formation is located at around 2.3 Å. The onset for bond formation in larger model systems occurs at slightly shorter bond distances as compared to the minimal system at the BLYP level of theory.

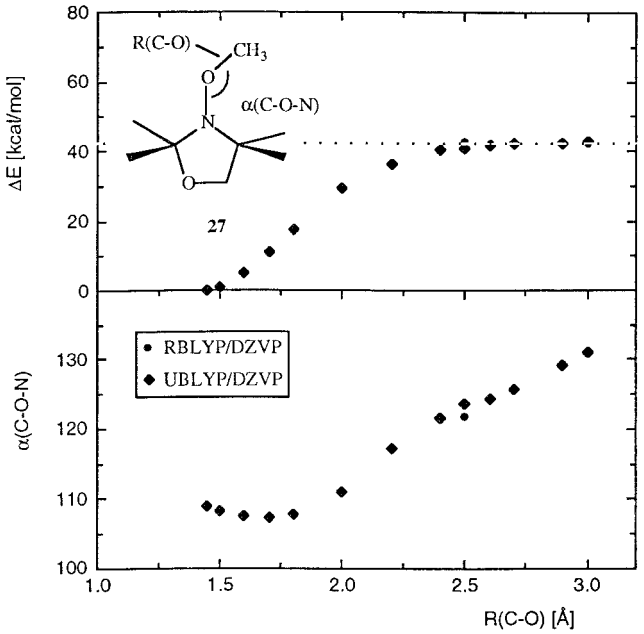

Figure 4. Relative energies as well as C−O−N angle deformation along the pathway for dissociation of **27** into methyl radical **23** and nitroxide radical **26**.

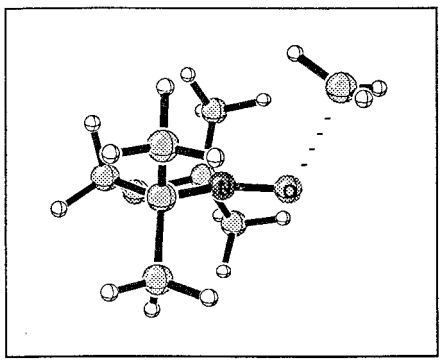

Figure 5. Structure of *N*-alkoxyamine **27** at a C−O bond distance of 2.2 Å.

angle at this stage is 117.2°. In comparison, Puts and Sogah, using PM3 calculations, found a transition state at a C−O distance of 2.07 Å and a C−O−N bond angle of 123.0° for DPPO, adding to 1-phenethyl radical.

It is interesting to compare our results to the classic work of Bürgi, Dunitz, Lehn, and Wipf, in which they used early ab initio calculations to look at the reaction pathway for the addition of hydride to the carbonyl group of formaldehyde.[57] They found, that at H−C distances of 2.5 Å, the H−C−O angle of attack was 126°, which decreased to 119° at 2.0 Å, to 118° at 1.5 Å, and finally to 109.5° at 1.12 Å. As in the carbon radical + nitroxide case, the hydride + formaldehyde calculations found no enthalpic barrier. Similarly, calculations on the addition of ammonia to formaldehyde at 2.0 Å gave an N−C−O angle of 105°, which compared favorably with bond angles of 107 ± 5° at 1.99 Å extracted from a series of crystal structures of amino carbonyl compounds.[58]

Conclusions

In the stereoselective coupling reaction between the sterically demanding chiral DPPO nitroxide and a series of stabilized secondary prochiral radicals, sterics make a significant contribution to the selectivity; however, there is a small but real electronic component. The effect of temperature was examined: higher stereoselectivity was obtained when the reaction was carried out at 0 °C than when it was started at −78 °C and allowed to warm to room temperature. ESR studies indicate that the generation of carbon radicals using the hydrazine method takes place at noticeable rates at 0 °C and higher.

The effects of solvent polarity and viscosity were examined. Although nitroxide trapping rates are affected by polar and protic solvents, this rate differential did not manifest itself into a change in stereoselectivity. The diastereoselectivity for the coupling of DPPO with tetralinyl radical was relatively constant at 4.8 ± 0.3 for toluene, THF, EtOH, and MeOH solvents. However, viscosity does play a role in stereoselectivity; selectivity was highest in nonviscous solvents (diethyl ether dr = 5.2:1) and was much poorer in highly viscous ethylene glycol (dr = 2.1:1). This viscosity dependence is interpreted as supporting evidence for the formation of an encounter complex in these non-diffusion-controlled reactions. In a less viscous solvent, the prochiral radical has more opportunity to reorient itself in a looser encounter complex to produce the more favorable coupling product as compared to a tighter encounter complex formed in a more viscous solvent.

Ab initio modeling studies predict that the C−O−N angle of attack of the carbon radical adding to the nitroxide is somewhat greater than 110° at a critical carbon−oxygen bond-forming distance of approximately 2.2 Å, although no transition state could be found. The angle of approach of the carbon radical adding to the N−O π bond of the nitroxide is very similar to that of a nucleophile adding to a carbonyl π bond.

Experimental Section

General. All reactions were run under nitrogen. Solvents were dried under nitrogen as follows: THF, diethyl ether, and toluene were distilled from sodium benzophenone. Dichloromethane was distilled from calcium hydride. Methanol was distilled from magnesium metal. Fuming hydrazine (anhydrous) was purchased from FisherBiotech (sequencing grade). Copper(II) chloride was dried over P_2O_5 by heating at 150 °C under house vacuum overnight. Reactions requiring sonication were performed by placing the reaction flask into a Fisher Scientific solid state/ultrasonic FS-14 bath cleaner; the height of the flask was adjusted so that the solution received maximum agitation. Flash chromatography was performed using Universal Scientific Inc. Silica Gel 63-200. IR spectra were recorded in deuterochloroform solution. Mass spectra were obtained using fast atom bombardment (FAB) on a VG ZAB-SE reverse geometry spectrometer with a VG 11/250 data system at the University of Illinois, and at UC Santa Cruz using a triple-quadrupole ESI spectrometer. Semipreparative HPLC was carried out using a Waters instrument with UV detection at 254 nm on a 150 × 4.6 mm Hasil 5 μm silica column. Elemental analysis was carried out by M−H−W Laboratories in Phoenix, AZ. Melting points are uncorrected.

$CuCl_2$ Oxidation of Lithium Enolates to Generate Prochiral Carbon Radicals: Coupling with DPPO. The following procedure is a typical example:

***tert*-Butyl 2-(*trans*-2,5-Dimethyl-2,5-diphenylpyrrolidine-1-oxy) Propionate (3).** A solution of *tert*-butyl propionate (61 μL, 0.400 mmol) in 1.4 mL of THF was cooled to −78 °C, and 2 M LDA in heptane/THF/ethylbenzene (266 μL, 0.532 mmol) was added. The mixture was stirred at −78 °C for 4 h. The C_2-symmetric nitroxide *trans*-2,5-dimethyl-2,5-diphenylpyrrolidine-1-oxyl (70.8 mg, 0.266 mmol) and $CuCl_2$ (anhyd, 57.3 mg, 0.426 mmol) were suspended in 1.7 mL of THF and cooled to −78 °C, and the enolate solution was added dropwise by cannula. The residues of enolate were washed with two

(57) (a) Dunitz, J. D.; Lehn, J. M.; Wipf, G. *J. Am. Chem. Soc.* **1974**, *96*, 1956−1957. (b) Bürgi, H. B.; Dunitz, J. D.; Lehn, J. M.; Wipf, G. *Tetrahedron* **1974**, *30*, 1563−1572.

(58) (a) Bürgi, H. B.; Dunitz, J. D.; Shefter, E. *J. Am. Chem. Soc.* **1973**, *95*, 5065−5067. (b) Bürgi, H. B.; Dunitz, J. D. *Acc. Chem. Res.* **1983**, *16*, 153−161.

0.5 mL portions of THF. The mixture was stirred at −78 °C overnight. It was then quenched with 2 mL of saturated $NaHSO_4$ at −78 °C, diluted with 15 mL of ether, and washed with 5 mL of saturated $NaHSO_4$ and 8 mL of saturated NaCl. The ether layer was dried over magnesium sulfate and filtered, and the volatiles were removed in vacuo to give a yellow oil which was purified by flash column chromatography (2 cm column, 95:5 hexane/ethyl acetate gradient) to yield 84 mg of colorless oil (80% yield). The major and minor diastereomers were obtained as a mixture in a 1.9:1 ratio, as elucidated by integration of the 500 MHz ^{1}H NMR spectrum in $CDCl_3$. Further purification was done by HPLC to obtain analytically pure samples of each diastereomer. TLC: 95:5 hexane/ethyl acetate, UV, *p*-anisaldehyde stain, $R_f = 0.4$. IR ($CDCl_3$): major diastereomer 2980, 2934, 1735, 1601, 1492, 1445, 1360, 1275, 1224, 1146, 1087, 1030 cm^{-1}; minor diastereomer 2981, 2936, 1737, 1601, 1492, 1445, 1370, 1265, 1222, 1162, 1134, 1084, 1030 cm^{-1}. ^{1}H NMR (500 MHz, $CDCl_3$): major diastereomer δ 7.22−7.83 (m, 10H), 3.86 (q, 1H, $J = 7$), 2.53−2.57 (m, 1H), 2.18−2.22 (m, 1H), 1.93−2.07 (m, 2H), 1.68 (s, 3H), 1.51 (s, 9H), 1.12 (s, 3H), 0.90 (d, 3H, $J = 7$); minor diastereomer δ 7.17−7.65 (m, 10H), 4.02 (q, 1H, $J = 7$), 2.54−2.60 (m, 1H), 2.16−2.24 (m, 1H), 2.02−2.08 (m, 1H), 1.88−1.96 (m, 1H), 1.51 (s, 3H), 1.41 (s, 3H), 1.23 (s, 9H), 1.07 (d, 3H, $J = 7$). ^{13}C NMR (125 MHz, APT, $CDCl_3$): major diastereomer δ 173.3 (s), 151.88 (s), 143.2 (s), 128.73 (d), 127.96 (d), 127.57 (d), 126.6 (d), 126.17 (d), 126.0 (d), 80.75 (s), 80.1 (d), 68.17 (s), 67.08 (s), 40.48 (t), 32.78 (t), 30.29 (q), 28.18 (q), 22.5 (q), 17.79 (q); minor diastereomer δ 172.53 (s), 151.99 (s), 143.54 (s), 128.42 (d), 127.99 (d), 127.66 (d), 126.55 (d), 126.0 (d), 125.86 (d), 80.66 (d), 80.55 (s), 70.37 (s), 69.19 (s), 40.43 (t), 33.23 (t), 29.56 (q), 27.9 (q), 25.1 (q), 17.6 (q). MS: major diastereomer *m*/*z* 395 [M$^+$], 266, 250, 236, 208, 131, 118, 103, 91, 84, 77, 57, 47; minor diastereomer *m*/*z* 395 [M$^+$], 266, 250, 236, 208, 131, 118, 103, 91, 84, 77, 57, 47. HRMS Calcd for $C_{25}H_{33}NO_3$: 395.2460 [M$^+$]. Found for major diastereomer: 395.2458. Found for minor diastereomer: 395.2458.

Methyl 2-(*trans*-2,5-Dimethyl-2,5-diphenylpyrrolidine-1-oxy) Propionate (4). The same procedure was followed to obtain 58 mg of pale yellow oil (55% yield). The major and minor diastereomers were obtained as a mixture in a 1.1:1 ratio, as elucidated by integration of the 500 MHz ^{1}H NMR spectrum in $CDCl_3$. TLC: 93:7 hexane/ethyl acetate, UV, *p*-anisaldehyde stain, $R_f = 0.44$. IR ($CDCl_3$): major diastereomer 2978, 1743, 1490, 1449, 1373, 1279, 1208, 1091 cm^{-1}. ^{1}H NMR (500 MHz, $CDCl_3$): major and minor diastereomers δ 7.18−7.77 (m, 20H), 4.22 (minor, q, 1H, $J = 7.5$), 3.97 (major, q, 1H, $J = 7$), 3.73 (major, s, 3H), 3.15 (minor, s, 3H), 2.52−2.62 (m, 2H), 2.14−2.30 (m, 2H), 1.90−2.06 (m, 4H), 1.60 (s, 3H), 1.59 (s, 3H), 1.37 (s, 3H), 1.15 (s, 3H), 1.14 (minor, d, 3H, $J = 7.5$), 0.97 (d, 3H, $J = 7$). ^{13}C NMR (125 MHz, APT, $CDCl_3$): major and minor diastereomers δ 174.00 (major, s), 173.76 (minor, s), 151.60 (s), 151.52 (s), 142.93 (major, s), 142.93 (minor, s), 128.47 (d), 128.25 (d), 128.05 (d), 127.83 (d), 127.60 (d), 127.52 (d), 126.68 (d), 126.54 (d), 126.15 (d), 125.95 (d), 125.81 (d), 125.75 (d), 125.56 (d), 125.40 (d), 80.56 (minor, d), 79.25 (major, d), 69.95 (minor, s), 68.49 (minor, s), 68.32 (minor, s), 67.26 (major, s), 51.44 (q), 51.05 (minor, q), 40.35 (minor, t), 40.21 (major, t), 33.17 (minor, t), 32.83 (major, t), 29.90 (major, q), 29.51 (minor, q), 23.99 (minor, q), 22.58 (major, q), 17.52 (major, q), 17.38 (minor, q). MS: m/z 354 [M + H]$^+$, 338, 266, 250, 236, 222, 157, 131, 118. HRMS Calcd for $C_{22}H_{27}NO_3$ 353.1990 [M$^+$]. Found: 353.1990.

Methyl 2-(*trans*-2,5-Dimethyl-2,5-diphenylpyrrolidine-1-oxy)cyclohexyl Acetate (5). The same procedure was followed to obtain 48 mg of colorless oil (76% yield). The major and minor diastereomers were obtained as a mixture in a 2:1 ratio, as elucidated by integration of the 500 MHz ^{1}H NMR spectrum in $CDCl_3$, which were purified further by HPLC. TLC: 95:5 hexane/ethyl acetate, UV, *p*-anisaldehyde stain, $R_f = 0.2$. IR ($CDCl_3$): 2928, 1743, 1492, 1446, 1373, 1275, 1202, 1172, 1059, 1029 cm^{-1}. ^{1}H NMR (500 MHz, $CDCl_3$): major and minor diastereomers δ 7.18−7.75 (m, 20H), 3.89 (minor, d, 1H, $J = 6$), 3.71 (major, s, 3H), 3.52 (major, d, 1H, $J = 7.5$), 3.15 (minor, s, 3H), 2.51−2.55 (m, 2H), 1.86−2.23 (m, 6H), 1.62 (minor, s, 3H), 1.57 (major, s, 3H), 1.55 (major, s, 3H), 1.15 (minor, s, 3H), 0.68−1.68 (m, 20H). ^{13}C NMR (125 MHz, APT, $CDCl_3$): major and minor diastereomers δ 173.44 (major, s), 172.88 (minor, s), 151.94 (minor, s), 151.66 (major, s), 144 (minor, s), 143.23 (major, s), 128.89 (d), 128.69 (d), 127.96 (d), 127.77 (d), 127.62 (d), 126.73 (d), 126.36 (d), 126.09 (d), 125.87 (d), 88.65 (minor, d), 86.77 (major, d), 71.98 (minor, s), 70.18 (minor, s), 68.39 (major, s), 67.41 (major, s), 51.15 (major, q), 50.89 (minor, q), 41.14 (major, t),40.93 (minor, t), 40.58 (minor, d), 40.47 (major, d), 34.49 (minor, t), 33.17 (major, t), 30.30 (major, q), 29.66 (minor, q), 29.30 (major, t), 29.19 (minor, t), 28.76 (major, t), 28.52 (minor, t), 26.47 (minor, t), 26.41 (major, t), 26.28 (t), 26.22 (t), 26.06 (t), 26.06 (t), 25.36 (minor, q), 22.49 (major, q). Elemental analysis: Anal. Calcd for $C_{27}H_{35}NO_3$: C, 76.92; H, 8.37; N, 3.32. Found: C, 76.88; H, 8.12; N, 3.25.

Methyl 2-(*trans*-2,5-Dimethyl-2,5-diphenylpyrrolidine-1-oxy)-phenyl Acetate (6). The same procedure was followed to obtain 45 mg of colorless oil (72% yield). The major and minor diastereomers were obtained as an inseparable mixture in a 1.4:1 ratio, as elucidated by integration of the 500 MHz ^{1}H NMR spectrum in $CDCl_3$. Further purification was done by HPLC. TLC: 95:5 hexane/ethyl acetate, UV, *p*-anisaldehyde stain, $R_f = 0.24$. IR($CDCl_3$): 2966, 1743, 1596, 1490, 1443, 1367, 1267, 1208, 1167, 1049, 1026 cm^{-1}. ^{1}H NMR (500 MHz, $CDCl_3$): major and minor diastereomers δ 7.02−7.88 (m, 30H), 5.09 (minor, s, 1H), 4.8 (major, s, 1H), 3.68 (major, s, 3H), 3.14 (minor, s, 3H), 2.56−2.68 (m, 2H), 2.21−2.29 (m, 2H), 1.96−2.12 (m, 4H), 1.71 (major, s, 3H), 1.51 (minor, s, 3H), 1.47 (minor, s, 3H), 1.02 (major, s, 3H). ^{13}C NMR (125 MHz, $CDCl_3$): major and minor diastereomers: δ 172.21 (major, s), 171.74 (minor, s), 151.74 (minor, s), 151.32 (major, s), 143.04 (major, s), 142.65 (minor, s), 136.34 (minor, s), 136.28 (major, s), 128.72 (d), 128.59 (d), 128.56 (d), 128.42 (d), 128.2 (d), 128.03 (d), 127.96 (d), 127.72 (d), 127.58 (d), 127.33 (d), 126.79 (d), 126.76 (d), 126.26 (d), 126 (d), 125.86 (d), 86.86 (minor, d), 85.2 (major, d), 69.64 (minor, s), 69.08 (major, s), 68.51 (minor, s), 67.84 (major, s), 51.88 (major, q), 51.51 (minor, q), 40.62 (minor, t), 40.32 (major, t), 33.37 (major, t), 33.06 (minor, t), 30.09 (major, q), 29.62 (minor, q), 23.71 (minor, q), 23.01 (major, q). MS: m/z 416 [M + H]$^+$, 266, 250, 236, 131, 118. HRMS Calcd for $C_{27}H_{29}NO_3$: 416.2226 (M + H). Found: 416.2232.

Methyl (2-(*trans*-2,5-Dimethyl-2,5-diphenylpyrrolidine-1-oxy))-4-methoxyphenyl Acetate (7). The same procedure was followed to obtain 28 mg of pale yellow oil (42% yield). The major and minor diastereomers were obtained as a mixture in a 1.65:1 ratio, as elucidated by integration of the 500 MHz ^{1}H NMR spectrum in $CDCl_3$. Further purification was done by HPLC. TLC: 95:5 hexane/ethyl acetate, UV, *p*-anisaldehyde stain, $R_f = 0.13$. IR ($CDCl_3$): major diastereomer 2955, 1737, 1602, 1508, 1443, 1373, 1255, 1167, 1091, 1026 cm^{-1}; minor diastereomer 2966, 1743, 1602, 1508, 1461, 1443, 1373, 1255, 1167, 1091, 1026 cm^{-1}. ^{1}H NMR (500 MHz, $CDCl_3$): major diastereomer δ 6.67−7.84 (m, 14H), 4.71 (s, 1H), 3.75 (s, 3H), 3.65 (s, 3H), 2.61−2.65 (m, 1H), 2.18−2.22 (m, 1H), 1.99−2.09 (m, 2H), 1.67 (s, 3H), 0.99 (s, 3H); minor diastereomer δ 6.83−7.62 (m, 14H), 4.98 (s, 1H), 3.81 (s, 3H), 3.13 (s, 3H), 2.52−2.57 (m, 1H), 2.19−2.26 (m, 1H), 1.93−2.06 (m, 2H), 1.48 (s, 3H), 1.43 (s, 3H). ^{13}C NMR (125 MHz, $CDCl_3$): major diastereomer δ 172.5 (s), 159.62 (s), 151.5 (s), 143.12 (s), 128.87 (d), 128.76 (d), 128.54 (d), 128.01 (d), 127.75 (d), 126.77 (d), 126.3 (d), 126.08 (d), 113.66 (d), 84.71 (d), 69.16 (s), 67.93 (s), 55.34 (q), 51.89 (q), 40.38 (t), 33.43 (t), 30.15 (q), 23.19 (q); minor diastereomer δ 172.06 (s), 159.9 (s), 151.86 (s), 142.742 (s), 129.13 (d), 128.64 (d), 128.59 (d), 128.06 (d), 127.64 (d), 126.85 (d), 126.02 (d), 125.91 (d), 113.86 (d), 86.31 (d), 69.69 (s), 68.55 (s), 55.42 (q), 51.53 (q), 40.67 (t), 33.05 (t), 29.66 (q), 23.86 (q). MS: major diastereomer m/z 446 [M + H]$^+$, 307, 266, 236, 179, 154, 118; minor diastereomer m/z 446 [M + H]$^+$, 266, 236, 179, 118. HRMS Calcd for $C_{28}H_{31}NO_4$: 446.2331 [M + H]. Found for major diastereomer: 416.2328. Found for minor diastereomer: 416.2334.

2-(*trans*-2,5-Dimethyl-2,5-diphenylpyrrolidine-1-oxy) Benzyl Nitrile (8). The same procedure was followed to obtain 34 mg of colorless oil (50% yield). The major and minor diastereomers were obtained as a mixture in a 1.4:1 ratio, as elucidated by integration of the 500 MHz ^{1}H NMR spectrum in $CDCl_3$. Further purification was done by HPLC. TLC: 95:5 hexane/ethyl acetate, UV, *p*-anisaldehyde stain, $R_f = 0.15$. IR ($CDCl_3$): 2966.2, 1460.7, 1378.4, 1260.9, 1096.4 cm^{-1}. ^{1}H NMR (500 MHz, $CDCl_3$): major and minor diastereomers δ 6.70−7.86 (m, 30H), 4.96 (major, s, 1H), 4.82 (minor, s, 1H), 2.62−2.80 (m, 4H),

2.09−2.30 (m, 4H), 1.87 (minor, s, 3H), 1.69 (major, s, 3H), 1.16 (minor, s, 3H), 1.06 (major, s, 3H). ^{13}C NMR (125 MHz, APT, $CDCl_3$): major and minor diastereomers δ 151.32 (s), 150.89 (s), 143.57 (minor, s), 142.63 (s), 132.92 (s), 132.44 (s), 129.79 (d), 128.91 (d), 128.66 (d), 128.53 (d), 128.46 (d), 128.22 (d), 128.22 (d), 127.93 (d), 127.82 (d), 127.32 (d), 127.04 (d), 126.89(d), 126.23 (d), 126.14 (d), 125. 94 (d), 119.15 (s), 119.11 (s), 75.11 (s), 74.81 (s), 74.75 (d), 74.55 (d), 69.27 (s), 68.03 (s), 40.36 (t), 38.49 (t), 33.33 (t), 33.22 (t), 31.21 (q), 30.19 (q), 28.54 (q), 22.92 (q). MS: m/z 383 $[M + H]^+$, 266, 236, 190, 131, 118. HRMS Calcd for $C_{26}H_{26}N_2O$: 383.2123 [M + H]. Found: 372.2121.

1-(*trans*-2,5-Dimethyl-2,5-diphenylpyrrolidine-1-oxy)isochromanone (9). The same procedure was followed to obtain 48 mg of pale yellow oil (45% yield). The major and minor diastereomers were obtained as a mixture in a 1.3:1 ratio, as elucidated by integration of the 500 MHz ^{1}H NMR spectrum in $CDCl_3$. TLC: 4:1 hexane/ethyl acetate, UV, *p*-anisaldehyde stain, $R_f = 0.39$. IR($CDCl_3$): 2966, 1755, 1708, 1604, 1443, 1255, 1085, 1026 cm^{-1}. ^{1}H NMR (500 MHz, $CDCl_3$): major and minor diastereomers δ 7.07−7.78 (m, 26H), 6.71 (d, 1H, $J = 7.5$), 6.38 (d, 1H, $J = 7.5$), 5.19 (d, 1H, $J = 14.0$), 4.85 (d, 1H, $J = 13.5$), 4.84 (d, 1H, $J = 14.0$), 4.82 (s, 1H), 4.76 (d, 1H, $J = 13.5$), 4.73 (s, 1H), 1.86−2.68 (m, 8H), 1.64 (major, s, 3H), 1.57 (minor, s, 3H), 1.29 (major, s, 3H), 1.16 (minor, s, 3H). ^{13}C NMR (125 MHz, APT, $CDCl_3$): major and minor diastereomers δ 168.85 (major, s), 168.43 (minor, s), 150.84 (major, s), 150.73 (minor, s), 143.52 (minor, s), 143.10 (major, s), 134.16 (major, s), 134.16 (minor, s), 131.53 (major, s), 131.42 (minor, s), 129.74 (d), 129.46 (d), 129.34 (d), 128.87 (d), 128.44 (d), 128.25 (d), 128.16 (d), 128.11 (d), 127.97 (d), 126.82 (d), 126.54 (d), 126.43 (d), 124.77 (d), 124.67 (d), 79.94 (major, d), 78.74 (minor, d), 73.05 (minor, s), 72.80 (minor, s), 70.72 (major, s), 70.23 (major, s), 69.71 (minor, t), 69.47 (major, t), 39.97 (major, t), 39.37 (minor, t), 35.04 (minor, t), 34.57 (major, t), 29.75 (major, q), 28.91 (minor, q), 26.62 (minor, q), 24.38 (major, q). MS: m/z 414 $[M + H]^+$, 266, 221, 190, 147, 131. HRMS Calcd for $C_{27}H_{27}NO_3$: 414.2069 [M + H]. Found: 414.2075.

Manganese Salen Method. For the synthesis of [*N*, *N*′-bis-(salicylidene)-1,2-ethanediaminato]manganese(III) chloride (**13**), see the Supporting Information.

Coupling of 1-(4-Nitrophenyl)ethyl Radical Generated by the Mn(salen) Method with DPPO To Form 1-(*trans*-2,5-Dimethyl-2,5-diphenylpyrrolidine-1-oxy)-1-(4-nitrophenyl)ethane (15). To a mixture of 4-nitrostyrene (22.4 mg, 0.150 mmol) and the C_2-symmetric nitroxide DPPO, *trans*-2,5-dimethyl-2,5-diphenylpyrrolidine-1-oxyl (40 mg, 0.150 mmol), in 0.74 mL of ethanol/ toluene (1:1) was added [*N*,*N*′-bis(salicylidene)-1,2-ethanediaminato]manganese(III) chloride (8 mg, 0.023 mmol), followed by di-*tert*-butyl peroxide (27.5 μL, 0.150 mmol) and sodium borohydride (11.3 mg, 0.300 mmol). The mixture was stirred at room temperature under nitrogen for 22 h. It was then evaporated to dryness and partitioned between 5 mL of dichloromethane and 8 mL of water. The aqueous layer was washed with 3 × 10 mL of dichloromethane. The combined dichloromethane layer was dried over magnesium sulfate, the solution was filtered, and the volatiles were removed in vacuo to give 85 mg of a dark brown, thick oil which was purified by flash column chromatography (1 cm column, 9:1 hexane/ dichloromethane gradient) to give 47 mg of colorless oil (75% yield). The major and minor diastereomers were obtained as an inseparable mixture in a 2.4:1 ratio, as elucidated by integration of the 500 MHz ^{1}H NMR spectrum in $CDCl_3$. TLC: 95:5 hexane/ethyl acetate, UV, *p*-anisaldehyde stain, $R_f = 0.37$. IR ($CDCl_3$): 2966, 1796, 1731, 1602, 1519, 1467, 1373, 1343, 1261, 1091, 1009 cm^{-1}. ^{1}H NMR (500 MHz, $CDCl_3$): major and minor diastereomers δ 8.13 (major, d, 2H, $J = 8.5$), 7.85 (minor, d, 2H, $J = 9.0$), 7.18 (major, d, 2H, $J = 9.0$), 7.06−7.72 (m, 20H), 7.03 (minor, d, 2H, $J = 8.5$), 4.50 (minor, q, 1H, $J = 6.5$), 4.33 (major, q, $J = 7$), 2.53−2.64 (m, 2H), 1.91−2.21 (m, 6H), 1.73 (minor, s, 3H), 1.36 (major, s, 3H), 1.28 (minor, d, 3H, $J = 6.5$), 1.14 (minor, s, 3H), 1.12 (major, s, 3H), 1.11 (major, d, 3H, $J = 6.5$). ^{13}C NMR (125 MHz, APT, $CDCl_3$): major and minor diastereomers δ 151.88 (minor, s), 151.67 (major, s), 151.63 (major, s), 150.98 (minor, s), 147.24 (major, s), 146.82 (minor, s), 143.18 (major, s), 143.14 (minor, s), 128.59 (d), 128.44 (d), 128.02 (d), 127.69 (d), 127.57 (d), 127.13 (d), 126.88 (d), 126.68 (d), 126.38 (d), 126.20 (d), 125.81 (d), 123.24 (major, d), 123.10 (minor, d), 81.17 (minor, d), 80.02 (major, d), 69.47 (major, s), 69.38 (minor, s), 68.60 (major, s), 68.01 (minor, s), 40.57 (minor, t), 40.48 (major, t), 34.21 (minor, t), 34.21 (major, t), 30.21 (minor, q), 29.65 (major, q), 23.73 (major, q), 22.98 (minor, q), 22.25 (minor, q), 21.69 (major, q). MS: m/z 417 $[M + H]^+$, 339, 309, 282, 266, 190, 152, 135, 119. HRMS Calcd for $C_{26}H_{28}N_2O_3$: 417.2178 [M + H]. Found: 417.2180.

1-(*trans*-2,5-Dimethyl-2,5-diphenylpyrrolidine-1-oxy)-1-(4-aminophenyl)ethane (16). The same procedure was followed to obtain 27 mg of pale yellow oil (39% yield). The major and minor diastereomers were obtained as a mixture in a 2.9:1 ratio, as elucidated by integration of the 500 MHz ^{1}H NMR spectrum in $CDCl_3$. TLC: 95:5 hexane/ethyl acetate, UV, *p*-anisaldehyde stain, $R_f = 0.13$. IR-($CDCl_3$): 3389, 3060, 2971, 2931, 2494, 1951, 1704, 1621, 1519, 1417, 1318, 1274, 1180, 1133, 1061, 1029 cm^{-1}. ^{1}H NMR (500 MHz, $CDCl_3$): major and minor diastereomers δ 7.25−7.69 (m, 20H), 6.94 (major, d, 2H, $J = 7.5$), 6.84 (minor, d, 2H, $J = 8$), 6.63 (major, d, 2H, $J = 8$), 6.49 (minor, d, 2H, $J = 7.5$), 4.16 (minor, q, 1H, $J = 6.5$), 4.14 (major, q, $J = 6.5$), 3.61 (br S, 2H), 2.47−2.64 (m, 2H), 1.87−2.21 (m, 6H), 1.58 (minor, s, 3H), 1.28 (major, s, 3H), 1.22 (minor, d, 3H, $J = 6.5$), 1.14 (major, s, 3H), 1.11 (minor, s, 3H), 1.06 (major, d, 3H, $J = 6.0$). ^{13}C NMR (125 MHz, APT, $CDCl_3$): major and minor diastereomers δ 152.56 (minor, s), 152.56 (major, s), 145.69 (major, s), 145.42 (minor, s), 144.1 (minor, s), 143.90 (major, s), 134.74 (major, s), 134.02 (minor, s), 128.67 (d), 128.05 (d), 127.91 (d), 127.78 (d), 127.46 (d), 126.59 (d), 126.45 (d), 126.15 (d), 126.06 (d), 125.96 (d), 125.75 (d), 114.75 (major, d), 114.75 (minor, d), 80.76 (major, d), 79.99 (minor, d), 68.84 (major, s), 68.84 (minor, s), 67.93 (major, s), 67.93 (minor, s), 40.63 (major, t), 40.42 (minor, t), 34.09 (minor, t), 33.82 (major, t), 30.00 (minor, q), 30.00 (major, q), 24.89 (minor, q), 23.48 (major, q), 21.66 (major, q), 21.55 (minor, q). MS: m/z 387 $[M + H]^+$, 282, 268, 252, 239, 224, 207. 190, 174, 157, 140, 120. HRMS Calcd for $C_{26}H_{30}N_2O$: 387.2435 [M + H]. Found: 387.2436.

1-(*trans*-2,5-Dimethyl-2,5-diphenylpyrrolidine-1-oxy)-1-phenylethane (14). The same procedure was followed to obtain 25 mg of a pale yellow oil (56% yield). The major and minor diastereomers were obtained as an inseparable mixture in a 3.4:1 ratio, as elucidated by integration of the 500 MHz ^{1}H NMR spectrum in CD_3CN. See compound **20a** for characterization.

Benzyl Hydrazine, Lead Dioxide Method for Generating Prochiral Carbon Radicals: Coupling to DPPO. For bromination of benzyl alcohols with Br_2/DIPHOS to give benzyl bromides, see the Supporting Information. The bromides were then reacted with hydrazine and then oxidized to form the prochiral carbon radicals. The following is a typical example.

1-(*trans*-2,5-Dimethyl-2,5-diphenylpyrrolidine-1-oxy)-1-phenylethane (20a). A mixture of (1-bromoethyl)benzene (205 μL, 1.5 mmol) and fuming hydrazine (940 μL, 30 mmol) was sonicated under nitrogen for 30 min. The cloudy solution was diluted with 30 mL of diethyl ether, and the hydrazine layer was washed with 10 mL of ether. The combined ether layer was washed with 20 mL of 10% potassium hydroxide solution followed by 10 mL of saturated sodium chloride solution. After drying over magnesium sulfate, the solution was filtered, and the volatiles were removed in vacuo to give 138 mg of a slightly yellow viscous oil. This oil was diluted with 0.6 mL of toluene. The C_2-symmetric nitroxide DPPO, *trans*-2,5-dimethyl-2,5-diphenylpyrrolidine-1-oxyl (67.4 mg, 0.253 mmol), and lead dioxide (121 mg, 0.506 mmol) were suspended in 0.6 mL of toluene, sonicated for 3 min under nitrogen, and cooled to −78 °C, and the benzyl hydrazine solution was added dropwise by cannula. The residues of benzyl hydrazine were washed in with two 0.3 mL portions of toluene. The mixture was allowed slowly to warm to room temperature, followed by filtration through Celite with dichloromethane rinses. The volatiles were removed in vacuo to give a thick, yellow oil which was purified by flash column chromatography (2 cm column, 95:5 hexane/ethyl acetate gradient) followed by a second column (1 cm, 95:5 hexane/ethyl acetate) to yield 58 mg of colorless oil (62% yield). The major and minor diastereomers were obtained as a mixture in a 2.5:1 ratio, as elucidated by integration of the 500 MHz ^{1}H NMR spectrum in CD_3CN. Further purification was done by HPLC to obtain an analytically pure sample of the mixture of diastereomers. TLC: 95:5 hexane/ethyl acetate, UV, *p*-anisaldehyde

stain, $R_f = 0.3$. IR ($CDCl_3$): 2966, 1461, 1379, 1261, 1091, 1014 cm^{-1}. ^1H NMR (500 MHz, CD_3CN): major and minor diastereomers δ 7.16−7.81 (m, 30H), 4.37 (major, q, 1H, $J = 7.0$), 4.30 (minor, q, 1H, $J = 6.5$), 2.58−2.79 (m, 2H), 2.05−2.36 (m, 6H), 1.73 (minor, s, 3H), 1.38 (major, d, 3H, $J = 6.5$), 1.35 (major, s, 3H), 1.19 (major, s, 3H), 1.14 (minor, s, 3H), 1.13 (major, d, 3H, $J = 7.0$). ^1H NMR (500 MHz, CD_3OD): major and minor diastereomers δ 6.96−7.69 (m, 30H), 4.22 (major, q, 1H, $J = 6.5$), 4.23 (minor, q, 1H, $J = 6.5$), 2.46−2.66 (m, 2H), 2.12−2.22 (m, 2H), 1.86−2.04 (m, 4H), 1.57 (minor, s, 3H), 1.22 (major, s, 3H), 1.20 (minor, d, 3H, $J = 6.5$), 1.04 (major, s, 3H), 1.03 (minor, s, 3H), 1.00 (major, d, 3H, $J = 6.5$). ^{13}C NMR (125 MHz, CD_3OD): major and minor diastereomers δ 153.61 (s), 153.36 (s), 145.71 (s), 145.71 (s), 145.05 (s), 144.84 (s), 129.78 (d), 129.04 (d), 128.97 (d), 128.81 (d), 128.54 (d), 128.44 (d), 128.11 (d), 127.80 (d), 127.69 (d), 127.48 (d), 127.32 (d), 126.94 (d), 82.73 (major, d), 81.88 (minor, d), 70.80 (minor, s), 69.75 (major, s), 69.75 (minor, s), 68.9 (major, s), 41.63 (major, t), 41.48 (minor, t), 34.95 (minor, t), 34.71 (major, t), 30.51 (major, q), 30.51 (minor, q), 25.02 (minor, q), 23.61 (major, q), 22.43 (minor, q), 22.26 (major, q). MS: m/z 372 $[M + H]^+$, 356, 267, 252, 190, 118, 105. HRMS Calcd for $C_{26}H_{29}NO$: 372.2327 [M + H]. Found: 372.2325.

1-(*trans*-2,5-Dimethyl-2,5-diphenylpyrrolidine-1-oxy)-1-(2,6-dimethylphenyl)ethane (20b). The same procedure was followed to obtain 27 mg of a whitish oil (32% yield). The major and minor diastereomers were obtained as a mixture in a 1.5:1 ratio, as elucidated by integration of the 500 MHz ^1H NMR spectrum in $CDCl_3$. TLC: 93:7 hexane/ethyl acetate, UV, *p*-anisaldehyde stain, $R_f = 0.5$. IR ($CDCl_3$): 2966, 1496, 1449, 1367, 1261, 1097, 1008 cm^{-1}. ^1H NMR (500 MHz, $CDCl_3$): major and minor diastereomers δ 6.72−7.73 (m, 26H), 4.63 (major, q, 1H, $J = 7$), 4.44 (minor, q, 1H, $J = 7$), 2.48−2.70 (m, 2H), 2.30 (major, s, 3H), 2.22 (minor, s, 3H), 2.07 (major, s, 3H), 1.95−2.25 (m, 6H), 1.82 (minor, s, 3H), 1.70 (minor, s, 3H), 1.28 (major, s, 3H), 1.28 (minor, s, 3H), 1.26 (major, d, 3H, $J = 7$), 1.08 (minor, s, 3H), 0.90 (minor, d, 3H, $J = 7$). ^{13}C NMR (125 MHz, $CDCl_3$): major and minor diastereomers δ 152.23 (major, s), 151.97 (minor, s), 143.80 (major, s), 143.74 (minor, s), 140.38 (major, s), 139.59 (minor, s), 136.09 (major, s), 135.90 (minor, s), 134.07 (major, s), 133.69 (minor, s), 130.74 (d), 130.51 (d), 128.69 (d), 128.59 (d), 127.88 (d), 127.61 (d), 127.40 (d), 126.87 (d), 126.56 (d), 126.48 (d), 126.37 (d), 126.26 (d), 126.20 (d), 126.17 (d), 125.84 (d), 125.75 (d), 79.71 (major, d), 76.78 (minor, d), 68.83 (minor, s), 68.83 (major, s), 67.79 (minor, s), 67.79 (major, s), 40.43 (t), 40.29 (t), 34.10 (t), 33.78 (t), 30.28 (q), 29.92 (q), 23.37 (minor, q), 23.20 (major, q), 22.36 (major, q), 21.91 (minor, q), 21.15 (major, q), 21,05 (minor, q), 19.20 (major, q), 18.80 (minor, q). MS: m/z 400 $[M + H]^+$, 309, 267, 252, 190, 155, 133,118. HRMS Calcd for $C_{28}H_{33}NO$: 400.2640 [M + H]. Found: 400.2642.

1-(*trans*-2,5-Dimethyl-2,5-diphenylpyrrolidine-1-oxy)-1-(4-trifluoromethylphenyl)ethane (20c). The same procedure was followed to obtain 86 mg of white solid (63% yield), mp 92−96 °C. The major and minor diastereomers were obtained as a mixture in a 3.5:1 ratio, as elucidated by integration of the 500 MHz ^1H NMR spectrum in $CDCl_3$. When the reaction was carried out at 0 °C for 4 h, the major and minor diastereomers were obtained as a mixture in a 4:1 ratio, as elucidated by integration of the 500 MHz ^1H NMR spectrum in $CDCl_3$. TLC: 7:1 pentane/methylene chloride, UV, *p*-anisaldehyde stain, $R_f = 0.5$. IR ($CDCl_3$): 2966, 2931, 1619, 1596, 1490, 1443, 1420, 1373, 1326, 1279, 1167, 1126, 1096, 1061, 1014 cm^{-1}. ^1H NMR (500 MHz, $CDCl_3$): major and minor diastereomers δ 7.01−7.72 (m, 28H), 4.41 (minor, q, 1H, $J = 6.5$), 4.29 (major, q, 1H, $J = 6.5$), 2.29−2.64 (m, 2H), 1.89−2.25 (m, 6H), 1.71 (minor, s, 3H), 1.34 (major, s, 3H), 1.28 (minor, d, 3H, $J = 6.5$), 1.13 (minor, s, 3H), 1.11 (minor, s, 3H), 1.09 (major, d, 3H, $J = 6.5$). ^{13}C NMR (125 MHz, APT, $CDCl_3$): major and minor diastereomers δ 152.11 (major, s), 151.24 (minor, s), 148.22 (major, s), 148.13 (minor, s), 143.38 (major, s), 143.38 (minor, s), 129.471 (major, q, ^2J (CF) = 31), 128.66 (d), 128.616 (minor, q, ^2J (CF) = 33), 128.52 (d), 128.00 (d), 127.69 (d), 127.60 (d), 127.52 (d), 126.80 (d), 126.70 (d), 126.60 (d), 126.28 (d), 125.93 (d), 125.78 (d), 125.02 (d), 124.91 (d), 124.88 (d), 124.78 (d), 124.42 (major, q, ^1J (CF) = 270), 124.39 (minor, q, ^1J (CF) =270), 81.03 (minor, d), 80.47 (major, d), 69.33 (minor, s), 69.25 (major, s), 68.35 (major, s), 68.07 (minor, s), 40.51 (major, t), 40.51 (minor, t), 34.24 (minor, t), 34.02 (major, t), 30.17 (minor, q), 29.67 (major, q), 23.67 (major, q), 23.29 (minor, q), 22.33 (minor, q), 21.77 (major, q). Elemental analysis: Anal. Calcd for $C_{27}H_{28}F_3NO$: C, 73.78; H, 6.42; F, 12.97; N, 3.19. Found: C, 73.57; H, 6.21; F, 13.30; N, 3.07.

1-(*trans*-2,5-Dimethyl-2,5-diphenylpyrrolidine-1-oxy)-1,2,3,4-tetrahydronaphthalene (20d). The same procedure was followed to obtain 14 mg of pale yellow oil (41% yield). The major and minor diastereomers were obtained as a mixture in a 5:1 ratio, as elucidated by integration of the 500 MHz ^1H NMR spectrum in $CDCl_3$. TLC: 93:7 hexane/ethyl acetate, UV, *p*-anisaldehyde stain, $R_f = 0.45$. IR-($CDCl_3$): 2940, 1462, 1376, 1260, 1093, 1001 cm^{-1}. ^1H NMR (500 MHz, $CDCl_3$): major and minor diastereomers δ 6.75−7.7.74 (m, 28H), 4.34 (major, t, 1H, $J = 3.5$), 4.08 (minor, dd, 1H, $J = 5.5, 4$), 2.51−2.82 (m, 6H), 1.67 (minor, s, 3H), 1.41 (major, s, 3H), 1.38 (major, s, 3H), 1.30 (minor, s, 3H), 1.32−2.30 (m, 14H). ^{13}C NMR (62.5 MHz, APT, $CDCl_3$): major and minor diastereomers δ 152.18 (minor, s), 151.50 (major, s), 143.94 (major, s), 143.72 (minor, s), 137.83 (major, s), 137.56 (minor, s), 136.43 (minor, s), 135.98 (major, s), 130.83 (major, d), 129.31 (minor, d), 128.55 (d), 128.44 (d), 127.73 (d), 127.64 (d), 127.43 (d), 127.38 (d), 126.95 (d), 126.49 (d), 126.31 (d), 125.99 (d), 125.89 (d), 125.64 (d), 125.22 (d), 124.76 (d), 77.40 (major, d), 76.03 (minor, d), 70.69 (major, s), 69.33 (major, s), 68.13 (minor, s), 67.24 (minor, s), 40.80 (minor, t), 40.27 (major, t), 35.15 (major, t), 33.46 (minor, t), 30.05 (minor, q), 29.95 (major, q), 29.33 (minor, t), 28.90 (major, t), 27.72 (major, t), 27.63 (minor, t), 24.28 (major, q), 23.20 (minor, q), 18.96 (minor, t), 17.96 (major, t). MS: m/z 398 $[M + H]^+$, 267, 252, 236, 190, 131, 118. HRMS Calcd for $C_{27}H_{29}NO_3$: 398.2484 [M + H]. Found: 398.2485.

1-(*trans*-2,5-Dimethyl-2,5-diphenylpyrrolidine-1-oxy)-indane (20e). The same procedure was followed to obtain 50 mg of a colorless oil (52% yield). The major and minor diastereomers were obtained as a mixture in a 5:1 ratio, as elucidated by integration of the 500 MHz ^1H NMR spectrum in $CDCl_3$. Further purification was done by HPLC to obtain an analytically pure sample of the mixture of diastereomers. TLC: 98:2 hexane/ethyl acetate, UV, *p*-anisaldehyde stain, $R_f = 0.25$. IR($CDCl_3$): 3154, 2978, 1813, 1796, 1602, 1467, 1378, 1261, 1091 cm^{-1}. ^1H NMR (500 MHz, $CDCl_3$): major and minor diastereomers δ 7.66−7.74 (m, 8H), 7.02−7.54 (m, 20H), 4.94 (major, t, 1H, $J = 5.0$), 4.75 (minor, dd, 1H, $J = 6.5, 5.0$), 2.77−2.95 (m, 2H), 2.52−2.67 (m, 4H), 2.02−2.28 (m, 6H), 1.72−1.74 (m, 4H), 1.71 (minor, s, 3H), 1.34 (major, s, 3H), 1.28 (minor, d, 3H, $J = 6.5$), 1.13 (minor, s, 3H), 1.11 (minor, s, 3H), 1.09 (major, d, 3H, $J = 6.5$). ^{13}C NMR (125 MHz, APT, $CDCl_3$): major and minor diastereomers δ 152.22 (major, s), 152.17 (minor, s), 144.80 (major, s), 144.15 (minor, s), 143.79 (minor, s), 142.72 (major, s), 128.61 (d), 128.66 (d), 128.48 (d), 128.25 (d), 128.02 (d), 127.89 (d), 127.71 (d), 126.42 (d), 126.29 (d), 126.18 (d), 126.12 (d), 126.07 (d), 126.00 (d), 125.92 (d), 125.51 (d), 124.63 (d), 124.58 (d), 87.39 (major, d), 86.08 (minor, d), 70.73 (major, s), 69.16 (major, s), 68.63 (major, s), 67.82 (minor, s), 40.68 (minor, t), 40.32 (major, t), 34.12 (major, t), 33.43 (minor, t), 32.98 (minor, t), 32.80 (major, t), 30.40 (minor, q), 30.26 (major, t), 30.00 (minor, t), 29.82 (major, q), 25.00 (major, q), 23.71 (minor, q). Elemental analysis: Anal. Calcd for $C_{27}H_{29}NO$: C, 84.56; H, 7.62; N, 3.65. Found: C, 84.34; H, 7.74; N, 3.47.

Coupling of 1-Tetralinyl Radical with *trans*-1,3-Dimethyl-1,3-diphenylisoindoline-1-oxyl (21) to form 1-(*trans*-1,3-Dimethyl-1,3-diphenylisoindoline-2-oxy)-1,2,3,4-tetrahydronaphthalene (22). The same procedure was followed using the C_2-symmetric nitroxide, *trans*-1,3-dimethyl-1,3-diphenylisoindoline-1-oxyl (**21**) (39.0 mg, 0.124 mmol), in place of DPPO to obtain 26 mg of a foamy, white solid (47% yield). The major and minor diastereomers were obtained as a mixture in a 3.2:1 ratio, as elucidated by integration of the 500 MHz ^1H NMR spectrum in C_6D_6. Recrystallization from hexane gave a white solid, mp 105−107 °C (dec). TLC: 5:1 pentane/methylene chloride, UV, *p*-anisaldehyde stain, $R_f = 0.33$. IR ($CDCl_3$): 2955, 2919, 1595, 1490, 1443, 1367, 1255, 1067, 1026 cm^{-1}. ^1H NMR (500 MHz, $CDCl_3$): major and minor diastereomers δ 6.76−7.58 (m, 36H), 4.21 (major, t, 1H, $J = 3.5$), 4.14 (minor, t, 1H, $J = 5.0$), 2.60−2.91 (m, 4H), 1.83−2.56 (m, 4H), 2.06 (minor, s, 3H), 1.39−1.70 (m, 4H), 1.62 (minor, s, 3H), 1.58 (major, s, 3H), 1.41 (major, s, 3H). [Note: The

methyl singlets at 1.58 and 1.41 ppm are seen only after cooling the NMR sample to −10 °C.] ^{13}C NMR (62.5 MHz, $CDCl_3$): major and minor diastereomers δ 148.67 (major, s), 148.14 (minor, s), 147.89 (s), 143.99 (major, s), 143.88 (s), 143.02 (minor, s), 137.67 (minor, s), 137.61 (major, s), 136.80 (major, s), 136.40 (minor, s), 131.93 (d), 129.79 (d), 129.46 (d), 128.92 (d), 128.65 (d), 128.53 (d), 128.50 (d), 128.17 (d), 127.98 (d), 127.87 (d), 127.73 (d), 127.44 (d), 127.17 (d), 127.10 (d), 127.03 (d), 126.86 (d), 125.50 (d), 124.83 (d), 123.74 (d), 123.61 (d), 77.02 (major, d), 76.66 (minor, d), 72.97 (major, s), 72.97 (major, s), 72.19 (minor, s), 72.07 (minor, s), 29.06 (minor, t), 29.14 (minor, q), 28.95 (major, q), 28.69 (major, t), 28.06 (major, t), 28.02 (minor, t), 20.69 (minor, q), 20.60 (major, q), 19.45 (minor, t), 17.94 (major, t). MS: m/z 446 $[M + H]^+$, 315, 300, 284, 269, 252, 238, 222, 206, 165, 131, 115. HRMS Calcd for $C_{32}H_{31}NO$: 446.2484 [M + H]. Found: 446.2483.

Acknowledgment. R.B. and N.N. thank the University of California, Santa Cruz, Faculty Research Funds and the National Science Foundation (Grant CHE-9527647) for providing financial support for this project. H.Z. thanks the Fonds der Chemischen Industrie for generous financial support. We thank Vladimir Chaplinski for the preparation of nitroxide **21**, Rodney Howden for the preparation of DPPO, and Glenn Millhauser and D. Joe Anderson for assistance with the ESR measurements. We thank Hans Fischer for insightful discussion.

Supporting Information Available: Preparation of DPPO **1**, preparation of Mn(salen) **13**, preparation of benzyl bromides **19b-e**, ^{1}H-NMR and ^{13}C-NMR spectra for **20b**, experimental procedures and ESR spectra for the variable temperature experiments monitoring both the hydrazine and enolate oxidation methods of radical generation (PDF). This material is available free of charge via the Internet at http://pubs.acs.org.

JA000520U